Facultad
de
Ciencias

PROSPECT OF FUTURE CTA OBSERVATION OF YOUNG SNR

(Perspectivas del futuro CTA en la observación de supernovas jóvenes)

Trabajo de Fin de Grado
para acceder al

GRADO EN FISICA

Autor: Estíbaliz Echevarría Guerrero

Director: Jose Ignacio Gonzalez Serrano

Co-Director: Andrea Giuliani

Octubre - 2018

Contents

List of Figures

List of Tables

Chapter 1

Introduction

Cosmic ray (CR) consist of charge particles, mainly protons ($\sim 90\%$) and the rest electron, helium and other heavier nuclei (Li,Be,B group). The origin of this particles is still under debate, but the analysis of their spectra show that their energy extends from below 1 GeV to around 10^{21} eV (see fig 1.1), describing by the following differential energy power-law:

$$\frac{dN}{dE} \sim E^{-\Gamma} \tag{1.1}$$

Where Γ is the spectral index. It describes the number of particles reaching the earth per unit time, surface, and solid angle, per unit energy interval.

The range of energies up to $3-4\cdot 10^{15}$ eV (called the knee) has an energy spectrum close to $\sim E^{-2.7}$ and it is believed to be originated within our galaxy. Around $E \sim 10^{18}$ eV, the spectrum flatters again ($\Gamma \sim 2.8$) [8] up to EeV range. The study and observation of the composition and the energy of this particles suggest that they have an extragalactic origin [9]. Above $5 \cdot 10^{19}$ eV the flux is expected to fall off due to the threshold energy of important interactions between cosmic rays particles and the cosmic microwave background (CMB). This phenomena is called the GZK effect (Greisen–Zatsepin–Kuzmin effect).

At the impact with the atmosphere, another flux of secondary particles is generated, and the analysis of those particles estimates that the population of cosmic ray on the galaxy must be around $10^{41} ergs \cdot s^{-1} = 10^{34}$ W [10]. This leaves the question if there is an energy source in the galaxy powerful enough to generate the CRs luminosity. The sites of acceleration of Cosmic Rays are not directly related to their arrival direction because to the diffusion of charged particles in interstellar magnetic fields, modifies the path of the particles. Since the 60s it has been suggested that supernova explosions are the only event powerful enough to generate the observed cosmic radiation. The main

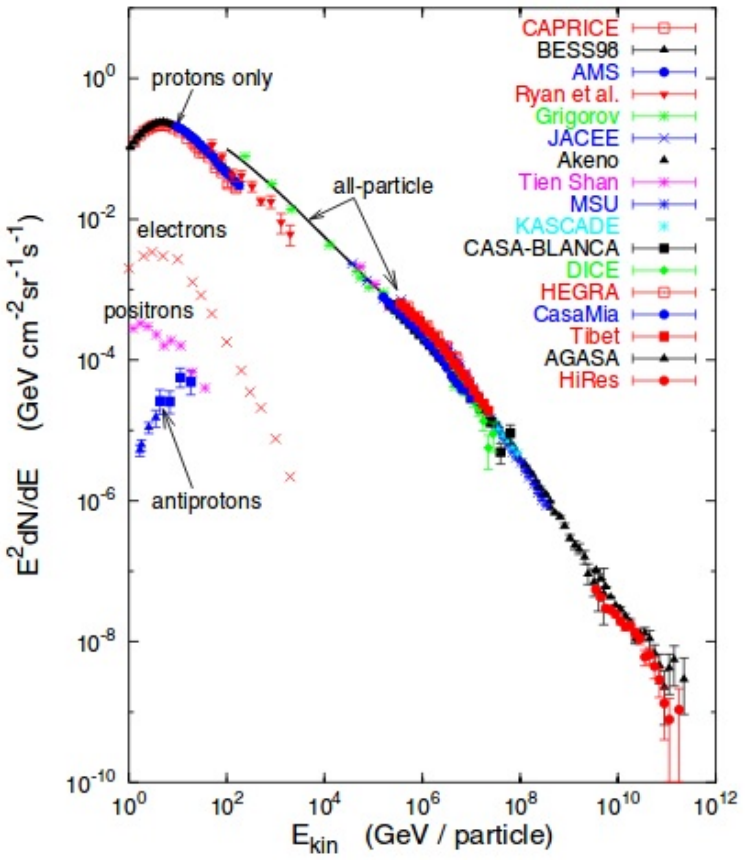

FIGURE 1.1: Global view of the cosmic ray spectrum measured by different experiments is plotted, together with the proton spectrum. The subdominant contributions from electrons, positrons and antiprotons measured by satellite experiments are also shown (from [1])

argument in favor of this hypothesis is that the amount of energy release ($\sim 10^{51}$ erg) and frequency of supernova explosions (1 every $\sim$ 30 years), are in perfect agreement with the observed CR luminosity if around 10% of the kinetic energy is used [10]. The second argument comes of the mechanism of diffusive shock acceleration (DSA) or Fermi acceleration.

The first apparent success of the DSA model was in explaining the general slope of cosmic ray spectra, $\sim E^{-q}$ which $q = \frac{r+1}{r-1}$ and r is the compression ratio felt by particles during the diffusion. It is expected that for strong shocks (shocks with Mach number $M > 1$), $r \sim 4$ and q=2. The evidence of synchrotron emission on SNR in the radio and X-ray band show presence of relativistic electron acceleration up to TeV energies. Also, gamma-ray measures made by satellites and ground telescopes in the GeV and TeV regime, shown proves of non-thermal activity not only by protons as well as electrons. Depending on the population of non thermal particles responsible of the gamma-ray emission, it is referred as hadronic or leptonic emission. Hadronic emission corresponds to neutral pion decay produced in collisions between relativistic nuclei and

the background plasma. Leptonic emission consists in radiation of electrons through inverse Compton scattering against the background photons.

The spectral index measured in most of SNR are larger than q=2 which still is a little flatter than the measures galactic CR spectrum of about $E^{-2.7}$ and larger than the spectrum predicted by the DSA model. In the TeV regime, this difference on the index could be due to the presence of a cut-off in the parent particle. On the other hand, the gamma-ray in the GeV regime could suffer losses due to the creation of secondary particles and losses due to the cooling time. A photon spectra of E^{-2} will be reduced by a factor of 0.5 because of those losses (will return $E^{-1.5}$), therefore does not explain the seeing spectra large than 2 observed in multiple SNR.

In the hadronic emissions, the $\gamma - ray$ spectrum has to be the same. In the leptonic scenario, instead, a contribution from non-thermal bremsstrahlung from $\sim GeV$ electrons must be added to the Inverse Compton one to fit the data. Also for bremsstrahlung emission, the photon spectrum is similar to the one of the parent particles, in turn implying that also GeV electrons must have a spectrum steeper than E^{-2} . It is worth recalling that in this region of the electron spectrum no cooling via synchrotron emission is effective, therefore protons and electrons are expected to show the same spectral index [11].

1.1 Non-linear DSA theories (NLDSA)

On the other hand, yet the DSA theory does not explain clearly the possible maximum energy that CR can achieve and the mechanism that accelerates does particles. Scientist have been working to developed theories to resolve that problems along with a correct spectrum prediction. Legage & Cesarsky (1983)[12] suggested that the maximum energy of cosmic rays in SNR is determined by an equal contribution of the acceleration rate and the lifetime of the SNR. Their results estimated that the shock has to propagate in a medium with a magnetic field greater than $100\mu G$ which is much larger that a typically interstellar values, which never exceeds 10^{14} eV [9].

The age of the remnant also limits the maximum energy achieved by CR, the shock velocity decreases with time ($E_{max} \sim t^{-1/5}$). Lucek and Bell (2000)[13] suggested that the diffusing high-energy particles ahead of the remnant shock generates Alfvén waves that impend the motion of the particles outside the remnant and generates fluctuations in the magnetic field that would provide the scattering needed. This would mean, that the most energetic particles would be generated very early, during the expansion phase when the strength of the self-generated magnetic field is proportional to the velocity

of the shock. Therefore, the effective maximum energy (the energy above which the spectrum falls very steeply) is no longer governed by the external magnetic field and varies slightly with the external density.

Drudy and Völk (1981) [14] suggested that the CR pressure modifies the shock structure, reducing the injection energy. Therefore, fewer CR are accelerated to relativistic energies, reducing the pressure at the same time and permitting the acceleration of more CRs. The plasma instabilities such as the Alfvén waves or NRH instability (non-resonant hybrid instability) among others could generate the enough magnetic strength to accelerate particles up to the PeV energies . The idea of non linear DSA models is to predict the back-reaction of the accelerated particles to induce, in the upstream, the formation of a precursor in which the fluid is slowed down because of the pressure in CRs diffusing around the shock. The net result is that particles with larger momentum, and in turn larger diffusion lengths, feel fluid compressions larger than 4. On the contrary, particles with mildly supra-thermal momenta only "see" a weaker sub-shock, with a compression ratio smaller than 4. This spread in the fluid compression ratio experienced by CRs leads to steeper spectra at low energies or flatter at high energies than E^{-2}. The NLDSA predicts that the more efficient the acceleration is, more pressure is induced to the CRs, affecting the spectra to values as $E^{-1.7/-1.5}$ around few GeV.

Also, it has to be considered that the CR spectra change during the propagation, in this case, through the galaxy. The widely accepted model for CR transport in the Galaxy, mainly based on CR isotope and secondary-to-primary compositions, suggests the residence time in the Galaxy as $E^{-\delta}$, with $\delta \sim 0.3$–0.6. The CR flux observed at Earth ($\propto E^{-2.75}$) has in fact to be proportional to the injection spectra $\propto E^{-q}$ multiplied by the Galactic residence time $\propto E^{-\delta}$, providing the constraint $q + \delta \cong 2.75$ and therefore implying $q = 2.2$–2.4. In addition, the smallest value $\delta \cong 0.3$ is preferred to account for the relatively small anisotropy observed in the direction of arrival of CRs above 1 TeV. Again, the spectra of CRs accelerated in SNRs should be steeper than those predicted in the DSA and NLDSA theories.

The solution to the index problem could be in the idea that the efficient amplification of the magnetic field via some plasma instabilities produced by the efficiency CR acceleration, would induce in the magnetic structures, acting as scattering centers for the CR diffusion, to achieve a non-negligible velocity with respect to the background fluid. This phenomenon may significantly alter the actual compression ratio felt by accelerated particles and, in turn, their spectrum and eventually the global shock dynamics. Some of this non-linear kinetic models seem to predict the expected levels of magnetic field amplification granted by streaming instabilities that lead to similar CR spectra that has been measured in young SNR ($E^{\sim -2.3}$)[15].

In summary, there have been developed multiple models to explain CR acceleration by SNR. But for now, only the Lucek and Bell model has proven to generate the large magnetic field necessary to scatter particles up to 1 PeV [16]. Also, there exist some observational proves of magnetic amplification that are consistent with non-linear DSA models (see Uchiyama et al. 2007, Helder et al. 2012). However, the index predicted seem to contradict the CR spectrum of the earth, gamma-ray observations, and another wavelength spectrum. A.R. Bell (2013)[16] presents different models that could resolve the problem of injection, proving the acceleration of CRs up to the PeV range is an important step to improve the theories of the origin of cosmic rays.

1.2 Detection of Cosmic Rays

From the prediction of theories and modelings it is known that a substantial fraction of the shock energy is transferred to the particles ($\sim 10\%$). When highly energy proton collides, produce neutral pions π^0 that quickly decay into two gamma rays [17] each having an energy of:

$$m_{\pi^0} \cdot c^2/2 = 67.5MeV \tag{1.2}$$

The normalized spectra of those gamma rays is therefore symmetric at that point or $\sim$ 200 MeV if the $E^2 \cdot F(E)$ representation is used [18]. This characteristic spectral feature (referred as pion decay-bump) uniquely identifies π^0-decay gamma ray coming from proton decay [2].

Yet, it was only possible to demonstrate the present of this pion-bump in IC443 and W44 supernova remnants. Both SNRs are surrounded by molecular clouds that enhanced the π^0 decay gamma emission due to more frequent proton-proton interaction. These middle age supernovas ($>$ 10000 years) show a very clear hadronic emission in the GeV band. Also, they show a high energy break at around 2 GeV for W44 and 20 GeV for IC443.

IC443 was detected in the GeV and TeV energy range by MAGIC and VERITAS. The centroid of the emission does not coincide, a fact that could be explained as the result of the escape of high energy CRs from the SNR shell and the interaction with the ambient medium [19]. W44 showed gamma-ray emission in the GeV regime due to interaction with a molecular cloud. Anyhow, even the acceleration of protons by SNR seem to be plausible, the maximum energy achieved by supernovas is not enough to accelerate particles to the PeV range (6 GeV for W44 around 1 TeV and 100 GeV for the two sources of IC443, see [20] and [21]). Another explanation is that gamma rays would have been produced by cosmic rays protons that had already left their shells and

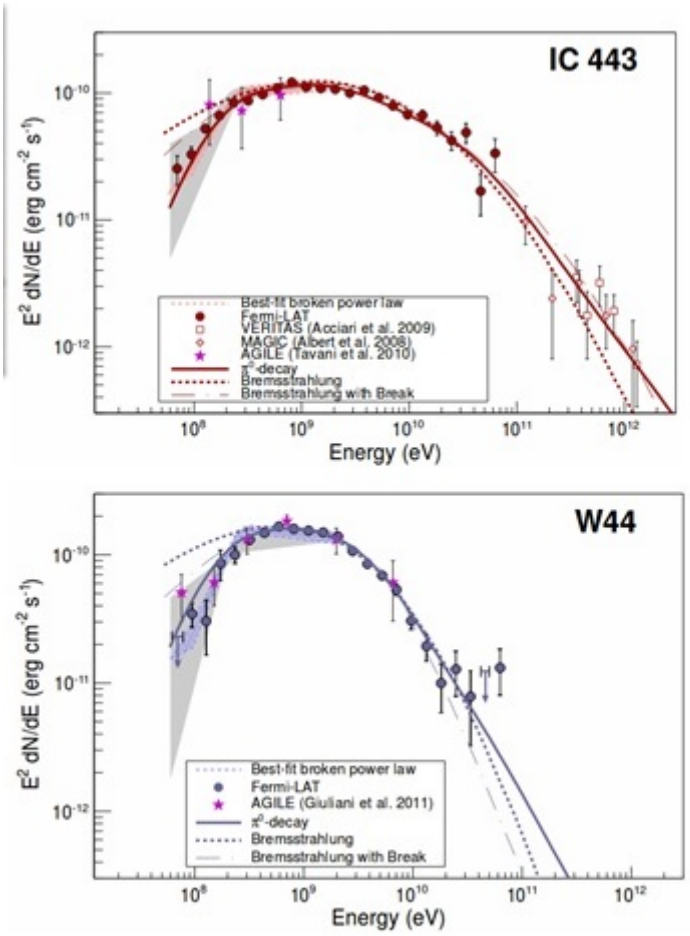

FIGURE 1.2: Gamma-ray spectra of IC 443 and W44 as measured with the Fermi-LAT, MAGIC and VERITAS . Solid lines denote the best-fit pion-decay gamma-ray spectra, dashed lines denote the best-fit bremsstrahlung spectra, and dash-dotted lines denote the best-fit bremsstrahlung spectra. The best fit show an energy break around 20GeV and 2GeV for IC 443 and W44, respectively. [2]

there are interacting with the molecular clouds. As said previously, the SNR particles inside the shell can provide their own mechanism to accelerate up to PeV. On the other hand, the shock velocity decreases with the age of the remnant. When the shock speed drops below 1000 km/s the magnetic field also decrease and the shell is unable to confine particles any longer. This happens after a few thousands years after the explosion, and moreover TeV-regime particles can not be observed but others at lower energies are expected to be seen [21].

There exists theoretical models that explain the gamma ray spectrum of SNR at very high emission (beyond 100 GeV). This has the inconvenient that it can be produced either from scattering of electrons off the ambient photon fields or interactions of protons with ambient matter, due to the same magnetic strength needed for Inverse Compton (IC) and π^0-decay. The key to distinguish between an electron or proton acceleration

seem to be in the analysis of the low energy regime. Magnetic fields can produce synchrotron loses on relativistic electrons, modifying the initial particle spectrum of the electrons producing a break. This break would be at an energy where the cooling time becomes comparable to the age of the source, and will follow a spectrum with 2 different index in the GeV and TeV regime:

$$\frac{dN}{dE} = N_0 \begin{cases} (\frac{E}{E_b})^{\Gamma_1} & E < E_b \\ (\frac{E}{E_b})^{\Gamma_2} & else \end{cases} \tag{1.3}$$

where E_b corresponds to the spectrum energy break and N_0 the normalization factor.

Synchrotron and IC have spectrums with the same shape but different energies, synchrotron dominates the X-ray regime while IC scattering dominates at GeV. Beyond 10 TeV the scattering should gradually fade out while synchrotron still appears from interactions of secondary electrons. The X-radiation produced by this secondary electrons has a very short lifetime compared to the age of the source. Therefore, they could be treated as instant radiation [22]. Inelastic pp-interactions and Bremsstrahlung emission can also produce energy loses. It is assumed that for low density mediums, inelastic pp scattering dominates over Bremsstrahlung. In conclusion, the analysis of gamma-ray spectrum starts with an accelerated power-law spectrum and then the probable photon losses are calculated.

1.3 Spectrum modelling

The spectrum of particles accelerated at the SNR shock is determined by the transport equation:

$$u(x)\frac{(\partial f(x,p)}{\partial x} = \frac{\partial}{\partial x}[D(x,p)\frac{(\partial f(x,p))}{\partial x}] + \frac{p}{3}\frac{du(x)}{dx}\frac{\partial f(x,p)}{\partial p} + Q(x,p) \tag{1.4}$$

Where u(x)is the fluid velocity in the wave reference frame, Q(x, p) accounts for particle injection, p momentum and

$$D(x) = \frac{v(p)}{3} r_L(x,p) \tag{1.5}$$

is the Bohm-like parallel diffusion coefficient for a particle with velocity v(p) and Larmor radius $r_L(x,p) = \frac{pc}{eB(x)}$ in the local, amplified magnetic field B(x).

Supposing that SNR is an efficient accelerator, CR modifies the f(x,p) low structure, making the shock more compressible and the spectrum of the accelerated particles harder $f_{0(p)} \sim p^{-\alpha}$ with $3.5 < \alpha < 4$. The maximum momentum of the accelerated particles is

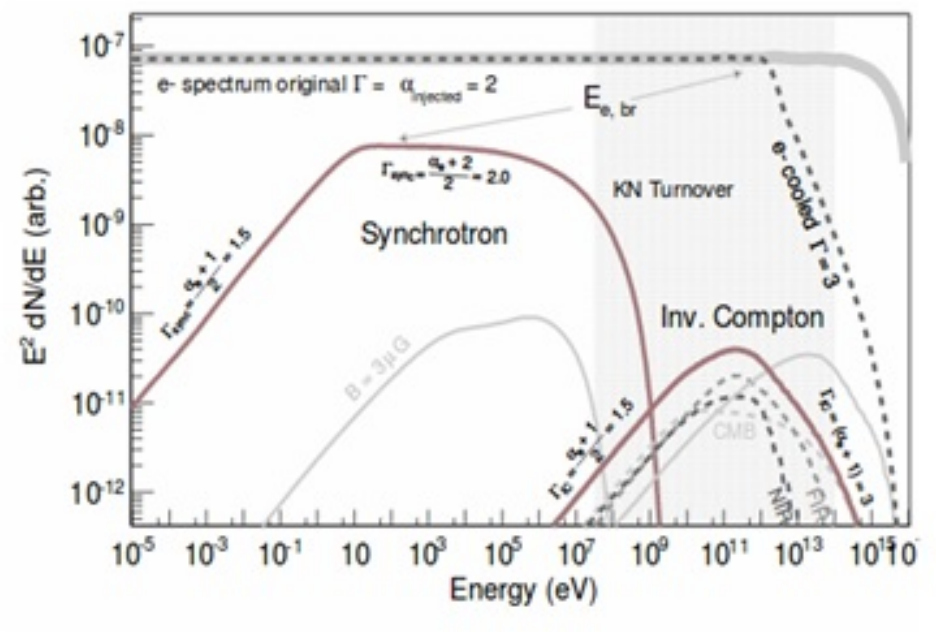

FIGURE 1.3: Spectral energy distribution of electrons with an initial power-law with $\Gamma = 2$ of a source with 1000 years, $B = 100\mu G$ at 100 pc. The dashed gray line shows the electron cooling model with a break around 1.2 TeV. Also the same break is apparent in the synchrotron spectrum and in the IC spectrum. At higher energies, its produce a high electron losses due to relativistic effects (Klein-Nishima regime). For $B = 3\mu G$ is also shown in light gray. The shaded region corresponds to the sensitive range of Fermi-LAT and IACTs detectors. The different Γ indicate the changes of the initial spectrum index α depending on the different energy loses [2]

determined by a simple confined condition: the diffusion length L_d of the particles can not exceed the characteristic size of the system R_{sh}. The maximum possible energies are achieved when the diffusion coefficient is proportional to p/B_{sh} with B_{sh} is the magnetic strength of the shock. This is called the Bohrn diffusion limit,and at this case the maximum momentum decrease with time as $p_{max}(t) \sim B_{sh} \cdot t^{-1/5}$ because also the magnetic field of the shock is expected to decrease with time, the drop of $p_{max}(t)$ is even faster. This implies that at any moment those particles that have reached the maximum momentum, quickly scape from the remnant generating a cutoff in the spectrum [23]:

$$\frac{dN}{dE} \sim E^{-\Gamma} e^{(\frac{-E}{E_0})^{\beta}} \tag{1.6}$$

At the TeV range, also gamma-ray spectrum can be measured due to interact of secondary particles synchrotron processes. The spectrum of this radiation at the cut-off is similar to an exponential cutoff with $\beta \approx \beta_{ee}/(2 + \beta_e)$ when β_e is the index for secondary electrons. This means that the secondary synchrotron radiation can be detected several decades beyond the cutoff energy [24].

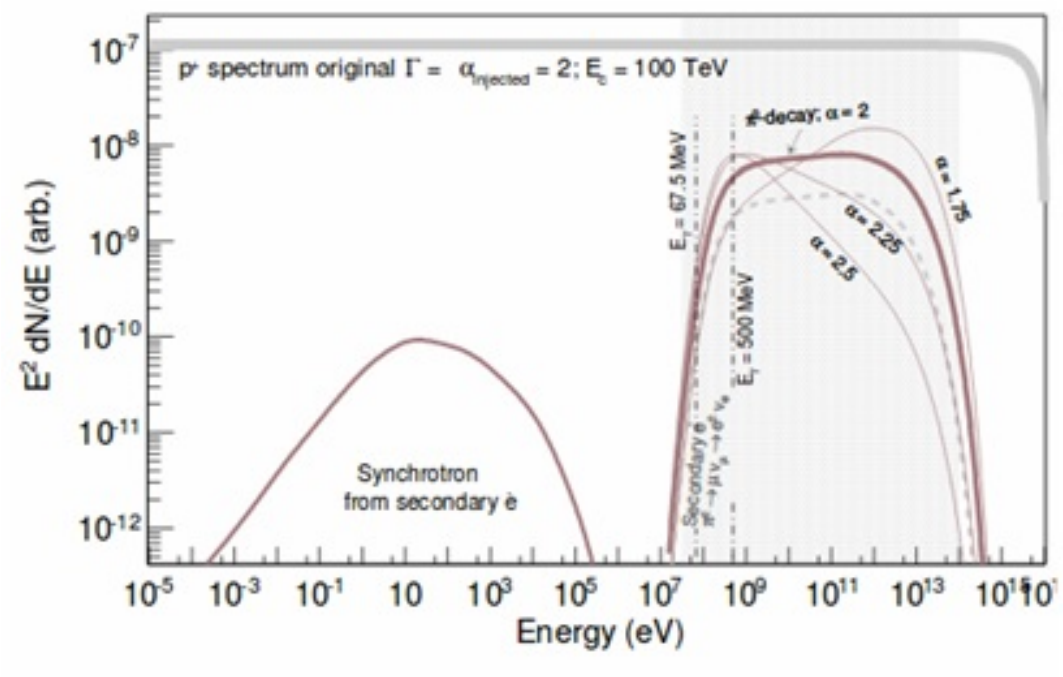

FIGURE 1.4: Spectral energy distribution of accelerated protons from a 1000 years source and $B = 30\mu G$. The dominant π^0 emission is represented as long as IC scattering for secondary electron-positrons interactions produced in $\pi^{+/-}$ decays and gamma ray resulting for inelastic collisions with interstellar material. The shaded region corresponds to the sensitive range of Fermi-LAT and IACTs detectors.[2]

1.4 Possible SNR candidates

The number of SNR detected at TeV energies is quite small and the proton can accelerate only up to PeV during a relatively short period of time, during the Bohm diffusive regime. Thus is expected to occur during the end of the free expansion and the beginning of the Sedov phase, for < 1000 years.

Only few number of detected SNR in the TeV regime seem to have around or less than 1000 years. The detection of very high gamma-ray emission is only possible with ground telescopes, because it requires large detection areas. It is expected a new array of Cherenkov telescopes that will cover the energy regime between 0.1 and 100 TeV. Studies of the performance of this new array suggested that it would be possible to measure a clearly spectra decay on type Ia and type IIb supernovas with less than 1000 years and up to 10kpc for Ia and up to 4kpc for type IIb [25]. Therefore, the possible candidates to measure CR is even lower. At this moment, the TeVCat catalog[1]list 5 SNR that exhibit shell-type morphology and have less or around 1000 years: Tycho (G120.1+01.4), SN1006 (G327.6+14.6), RXJ1713.7-3946 (G347.3-00.5), Cassiopeia

[1]tevcat.uchicago.edu

A (G111.7-02.1). SNRs like HESS J1721-347, J1912-101, J1534-571 and J171614-518 could be good candidates for PeV searching, but their age, distance and morphology seem not to be clearly resolve yet. However, more studies of their spectrum and morphology could change this. The cases of Kepler (G4.5+06.8) and G1.9+0.3 could also be good candidates for VHE gamma-ray. For G1.9+0.3 HESS telescope could have found synchrotron radiation that could indicate either acceleration of protons and/or electrons at VHE energies [26]. For Kepler, not clear gamma-ray spectrum was able to be measured and it seems to be due to its location, distance, and age[27].

The measures at different wavelengths of Tycho, Cassiopeia A, SN1006 and RXJ1713.7-3946 have permitted to estimate magnetic field values and the maximum energy achieved the accelerated particles. In the case of RXJ1713.7-3946 there are still doubts whether its emission has an hadronic or leptonic but it was possible to identify a clearly cut-off spectrum due to the proximity and brightness, of around 6.7 TeV (Abdalla et al. 2016[28]). Due to its age ($\sim$ 1600 yrs), is not expected to find cut-offs around 100 TeV in the future, the same for SN1006 which some models predict a cut-off detection $<$ 60 TeV. The best possible chance is to find PeV acceleration is to focus on the youngest SNR at the moment and hope that will "catch" them while there are still accelerating particles.

Chapter 2

Gamma-ray detection and Analysis

To detect and measure the emission of gamma-ray fluxes astronomers use different type of detectors, that mainly can be classified in two types: space-base and ground base telescopes.

2.1 Space-base Telescopes

The main base space telescope is the *Fermi gamma-ray Space Telescope* launched in 2008. Its main instrument is the Large Area Telescope (LAT) that covers observations in the energy range between $\sim$ 20 MeV and 300 GeV. The effective collection area of the LAT is about 0.65 m^2 above 1 GeV and an angular resolution of 0.8^o at 1 GeV, better than 0.2^o above 10 GeV . Another important space telescope is AGILE (Astrorievelatore Gamma ad Immagini Leggero). It consists on a Gamma Ray Imaging Detector (GRID) sensitive in the 30 MeV - 50 GeV energy range, a SuperAGILE (SA) hard X-ray monitor sensitive in the 18–60 keV energy range, a Mini-Calorimeter (MCAL) non-imaging gamma-ray scintillation detector sensitive in the 350 keV - 100 MeV energy range [3]. The good thing about space base telescopes is that they directly detect the gamma burst and that they can be calibrated in the laboratory before being launched. The problem is that they do not seem to be very efficient for energies above 100GeV due to a limitation in their detection areas [24].

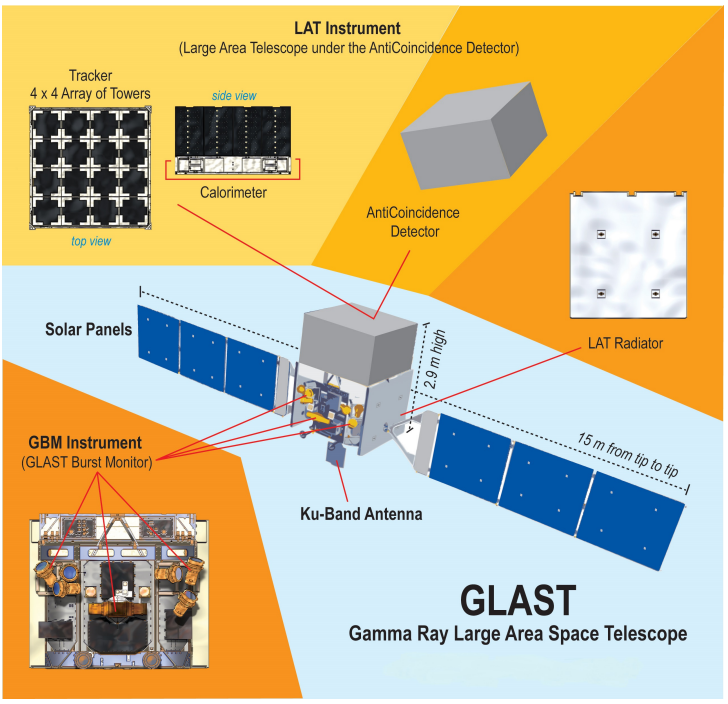

FIGURE 2.1: Schematic illustration of the GLAST satellite. The Gamma-ray Burst Monitor (GBM) (formerly GLAST Burst Monitor) detects sudden flares of gamma-rays produced by gamma ray bursts. The tracking section of the LAT consists of 36 layers of silicon strip detectors interleaved with 16 layers of tungsten foil. The calorimeter is composed of CsI crystals that measured the total energy of the pair positon-electron created in the tracking by photon incidence. Surrounding the tracker there is anti-coincidence detector formed by plastic scintillators read out by photomultiplier tubes [3]. (photo from https://www.nasa.gov/mission_pages/GLAST/multimedia/glast_vector.html)

2.2 Ground base Telescopes

The ground base telescopes observe those gamma rays by detecting Cherenkov photons from electromagnetic cascades induced by gamma rays on their interaction with the atmosphere. Two techniques exist to detect those air showers, the *Imagine Atmospheric Cherenkov Telescopes* (IACTs) detects directly the Cherenkov light generated in the atmosphere. And the *Water Cherenkov Detectors* (EAS), in this case the particles are detected through the light that it is emitted when they pass a tank of purified water located at high altitudes.

When photons interact with the atmosphere, a pair of electron a positron is created. The pair travel through the atmosphere at very high speed, higher speed than the speed of light in the atmosphere medium. This disrupt the electromagnetic field making the medium electrically polarized. Therefore, the excess of energy is eliminated emitting radiation in the form of light. The shape of the air showers retains the original direction of the incident gamma ray, so the IACTs large optical reflectors are equipped with

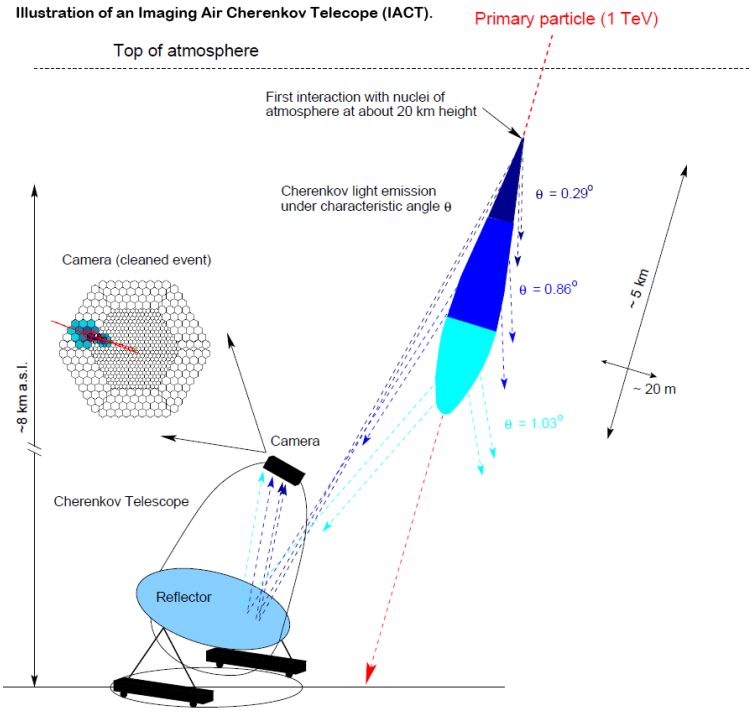

FIGURE 2.2: Schematic of the detection of gamma-ray induced showers with the IACT. An incident high-energy gamma ray interacts in the atmosphere and generates an air shower positrons and electrons. The number of shower particles reaches a maximum at about 10 km height, and then it dies. Since the shower particles move at essentially the speed of light, they emit the Cherenkov light in the form of a cone with maximum angle $\theta \sim 1$. The light is reflected by the mirrors of the telescope and focused at the so-called camera. The camera consists of multipliers which turn the photons to electrical signals to be processed.[4]

pixel cameras to record te incoming photons. The gamma ray fluxes also are very weak and only last a few ns, to compensate this and reduce the background, multiple optical reflectors of 10m of size are used separated 100 for each other, providing huge detection areas ($\geqslant 3 \cdot 10^4 m$) and reducing the effective energy threshold which improves the resolution of the gamma rays and reduce the background [24].

Currently, three IACT observatories are operating: HESS (High Energy Stereoscopic System) located in Namibia, MAGIC (Major Atmospheric Gamma-ray Imaging Cherenkov Telescopes) in Las Palmas island and VERITAS (Very Energetic Radiation Imaging Telescope Array System) in Arizona. They achieved to detect minimum fluxes of around $10^{-13} erg/m^2$ covering the energy range between approximately 30 or 50 GeV to 50 TeV [24]. In the future, it is expected to increase their sensitivity one order of magnitude that will extent the detection energy range from 10 to 100 TeV or even higher. To do so, new array of Cherenkov telescopes (CTA) it is being built employing 3 new sizes of telescopes at the same locations and a new IACT observatory in Chile. The large size telescope (LST) of around 24m of diameter will record the lower range, the medium size telescope (MST) of around 12m of diameter will operate in the 1 TeV

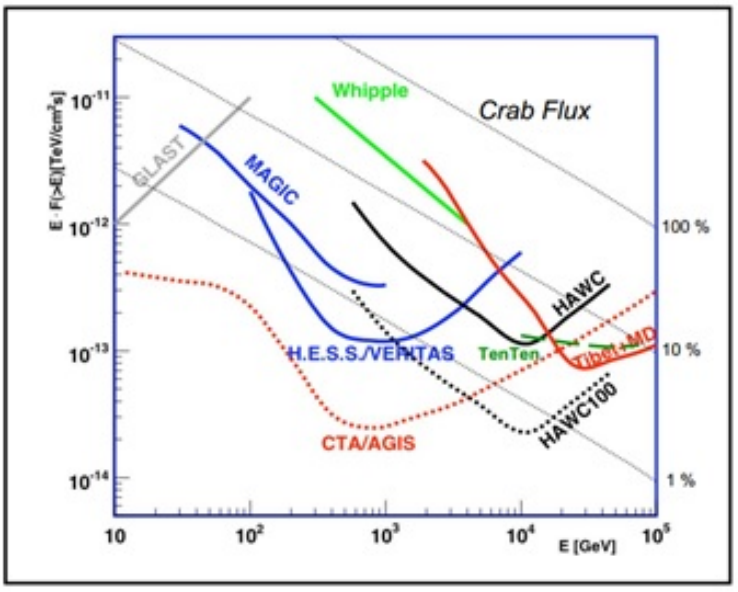

FIGURE 2.3: Point-source sensitivity of current and future gamma-ray observatories to constant sources. For pointed instruments (HESS/VERITAS) the sensitivity is shown for a 50h exposure to a single source. For all-sky instruments such as GLAST, Tibet+MD, HAWC and HAWC100 the sensitivity shown indicates the level at which these instruments will survey the sky that is visible to them (typically $2\pi sr$, 4π for GLAST) after five years of operation.[5]

range and the small size (SST) between around 4-7 m of diameter that will operate in the higher energy range. The detection area will also increase (around 1km2) and the angular resolution (around 0.02^o [3]] or 0.03^o [5] at 1 TeV) By the improvement of the sensitivity it is expected in the future to detect new large gamma-ray sources both in north and south hemisphere in the TeV regime that will allow to identify new possible sources of cosmic ray acceleration.

Water detectors are less sensitive to point sources than IACTs, but have the advantage that they can monitored the sky at all hours. IACTs operate at dark hours (night without moon) to reduce the background light. Also for large sources their sensitivity is much better, groups like Milagro, $AS\gamma$ and Tibet-III detector have demonstrated their sensitivity with detections of the Crab Nebula [5] and the detection of new sources in the galactic plane [24]. The water detectors have showed capabilities that can be used along with IACTs in the study of gamma-sky at the TeV regime.

2.3 Simulation tools

To allow the analysis of gamma-ray event a standardization in the data formats have been made along with a development of software package that gather all those events and permit their analysis.

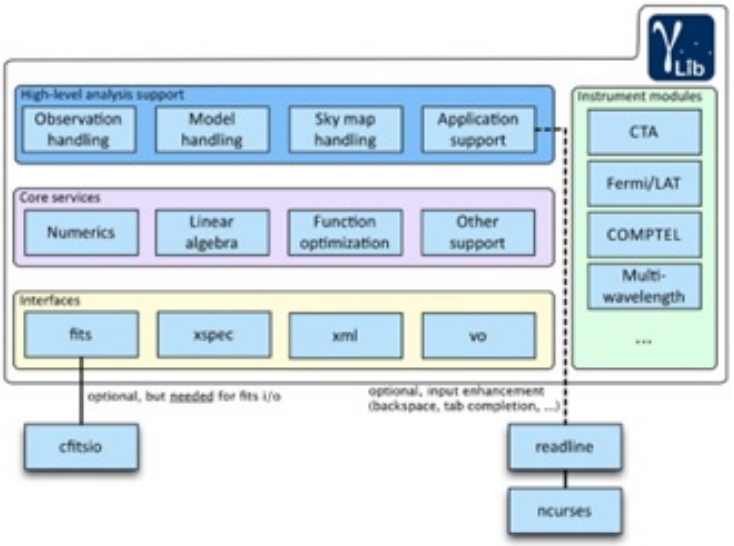

FIGURE 2.4: Scheme of gammaLib organization. The software layers are represented in different colors. In each layer, in blue, the modules those included and optionally needed for manage files.[6]

GammaLib is written mostly in C++, it contains all the functions needed for the analysis of gamma-ray data. Only relies on cfitsio library from **HEASARC** that is used to read and write data files in **.fits** format (see:https://heasarc.gsfc.nasa.gov/fitsio/fitsio.html) It treats the gamma-rays events as abstract representations so they do not depend on the characteristic of the instrument employed of the measures or in the format of data and instruments respond functions. GammaLib is organized in four software layers, each of them comprise several modules: a layer for interment analysis, for instrument independent services, an interface layer that allows handling of data in: **.fits**, **.xml**, **.xspec** and **.vo** formats and instrument layer for handle data obtained with any kind of gamma-ray telescope.

The *ctools* software provides the necessary tools for the analysis of IACT events. The software works with list of reconstructed events and IACT respond functions allowing the creation of images, spectra, and light curves of gamma ray sources, providing the results in **FITS** format. *Ctools* also provides the tools that allow simulate future CTA just by introducing the instrument response functions, which relates the gamma-ray intensity arriving at Earth as a function of photon properties. Those calibrations are save following the **HEASARC** calibration data base (**CALDB**) format, where the instrument response functions are specified for *ctools* usage by the *caldb* and *irf* parameters. The first gives the calibration name and the second the name of the response function (IRFs) (see:http://heasarc.gsfc.nasa.gov/docs/heasarc/caldb/caldb_intro.html). *Ctools* are shipped with response functions for the northern and southern arrays, with variants that have been optimized for exposure times of 0.5 hours,

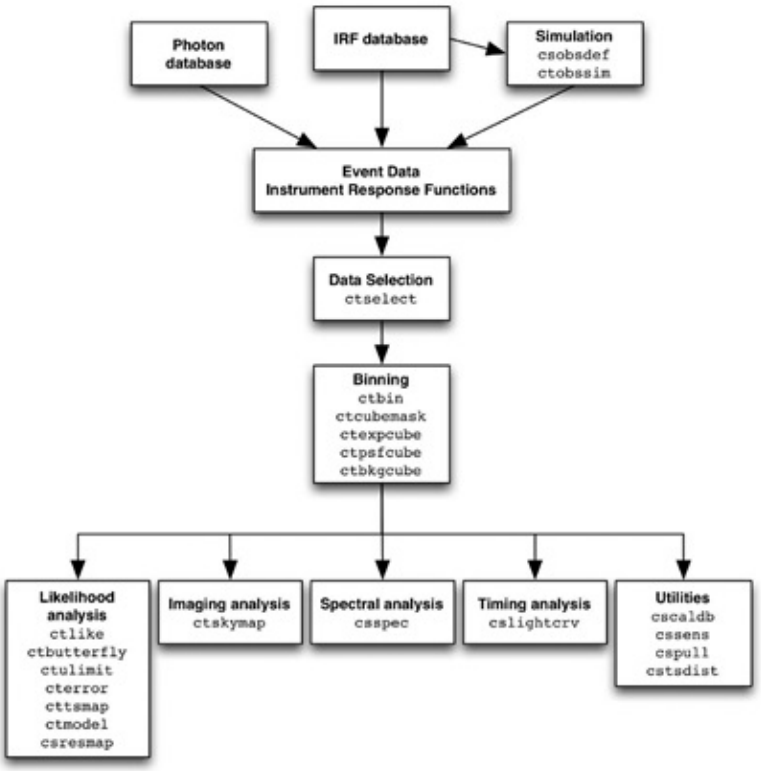

FIGURE 2.5: Summary of the available tools release in 1.0 ctools package, grouped according to functionality and arranged according to their typical usage.[7]

5 hours, and 50 hours. A summary of the available tools for spectra analysis can be found at the figure 2.5, the package is in continuous updating. For further information about *GammaLib* and *ctools* packages see [11], [29], [7], [30] and [31].

The aim of this work is to evaluate the capability of CTA to perform spectral studies of shell type SNR. As it was explained in the first part, the study of spectral features with good accuracy can help to determine the origin of gamma ray emissions. Also, the ability on determining cut-off in the spectra is required to obtained the maximum energy of the accelerated particles. We believe that the best candidates for searching accelerated cosmic rays are Tycho, Cassiopea A and Kepler supernovas, because of their age (< 500 years) type, and distance. Multiwavelength observations of Kepler SNR suggested a distance of at least 6 kpc [27] which is higher than the horizon of detectability stimated for this kind of supernova (~ 5 kpc). For these three, we simulated their spectrum using the *ctools* software package. We used *ctobssim* to generate the observation events, *cspec* script to reproduce the flux spectrum and *ctlike* to fit the simulation to determine their indexes and cut-offs and to perform a maximum likelihood fit to obtained the fitting cut-off energy. Also, *ctskymap* was used to generate a VHE photon maps of the events.

2.3.1 ctobssim

ctobssim is an simulation tool that creates event files which contains the reconstructed incident photon direction in sky coordinates, the reconstructed energy, and arrival direction for each VHE photon detected in the field of view (FoV). The software needs to introduce the coordinates of the source, the desired FoV of the instrument and the IRF. The CTA website provide "2Q" array configurations which, as explained previously, are save in the *caldb* folder of *ctlike*. Two calibration databases were used for the simulation: *prod2* which contains the respond functions for the northern and the southern hemisphere optimized for 0.5, 5 and 50h point source observations. And *prod3b* which contains the same but optimized for a zenith angle of 20 degrees. To simulate events, also source and a background models are needed, those must be defined in a XML file. The modeling of the celestial source is given by a factorized function in where the spatial, spectral, and temporal components of the source are defined. The background component is modelling as a radial gaussian function in squared off set angle (off set angle is defined as the angle between pointing and measured event direction).

Ctools has available different spatial and spectral models (see: http://cta.irap.omp.eu/ctools/users/user_manual/getting_started/models.html?highlight=model). For spatial we only considered point source emission for the remnants. At this work, we are only interested in reproducing spectra of single power laws, single power laws with exponential cut-offs and broken power-laws, those are defined by the following expressions:

$$\frac{dN}{dE} = N_0 \frac{E}{E_0})^{\Gamma} \tag{2.1}$$

$$\frac{dN}{dE} = N_0 (\frac{E}{E_0})^{\Gamma} e^{E/E_{cut}} \tag{2.2}$$

Where N_0 is the normalization factor and E_{cut} the cut-off energy. By default, E_0 always have a 1TeV value.

$$\frac{dN}{dE} = N_0 \begin{cases} (\frac{E}{E_b})^{\Gamma_1} & E < E_b \\ (\frac{E}{E_b})^{\Gamma_2} & else \end{cases} \tag{2.3}$$

where E_b corresponds to the spectrum energy break and N_0 is the normalization factor.

FIGURE 2.6: XML created for simulated Tycho spectrum. The spatial model is defined as point source type.The values set as prefactor, index and cut-off energies correspond to the parameters N_0, Γ and E_{cut} of (2.1) and (2.3) expresions. The energy is given in MeV and the parameter set with *free=0* means that they are fixed while those with *free=1* could be change during the fitting. The parameter *tscalc=1* is used to show the test statistic calculated during the fitting part.

2.3.2 ctlike

ctlike tool was used to fit the simulated data, previously done with *ctobssim*. By default, it uses Poisson statistics to perform maximum log-likelihood computation. This is defined by:

$$-\ln L_i(M) = \sum_k (e_{k,i}(M) - n_{k,i} \ln e_{k,i}(M)) \tag{2.4}$$

Where k is the number of events in bins, $n_{k,i}$ the number of events in a bin k obtained during an observation i and $e_{k,i}$ the predicted number of events for the model M in bin k of the observation i.

The fitting can be done using the binned or the unbinned mode. At the binned mode, the events are into 200x200x20 count cubes bin. A counts cube is a 3-dimensional data cube, comprised by Right Ascension (or Galactic longitude), Declination (or Galactic latitude), and energy. The number of events generated are less than the number of bins contain in the count cubes, therefore the amount of operations needed to perform are less and more precise. *ctlike* also computes the test statistics (TS) value, which compares the maximum likelihood value for a full model M and the maximum likelihood

```
<?xml version="1.0" encoding="ISO-8859-1"?>
- <source_library title="source library">
source library
    e tscalc="1" ts="1246.270" type="PointSource" name="Tycho">
      pectrum type="ExponentialCutoffPowerLaw">
        <parameter name="Prefactor" free="1" max="1000" min="1e-07" scale="1e-19" error="0.725968133016364" value="5.13090114362928"/>
        <parameter name="Index" free="1" max="5" min="0" scale="-1" error="0.106136564200381" value="1.95484916745322"/>
        <parameter name="CutoffEnergy" free="1" max="1000" min="0.01" scale="1000000" error="0.212925426539474" value="1.41216606337073"/>
        <parameter name="PivotEnergy" free="0" max="1000" min="0.01" scale="1000000" value="1"/>
      </spectrum>
    - <spatialModel type="SkyDirFunction">
        <parameter name="RA" free="0" max="360" min="-360" scale="1" value="6.34"/>
        <parameter name="DEC" free="0" max="90" min="-90" scale="1" value="64.13"/>
      </spatialModel>
  </source>
- <source type="CTAIrfBackground" name="CTABackgroundModel" instrument="CTA">
  - <spectrum type="PowerLaw">
      <parameter name="Prefactor" free="1" max="1000" min="0.001" scale="1" error="0.00230621080725156" value="0.996851648224662"/>
      <parameter name="Index" free="1" max="5" min="-5" scale="1" error="0.00146302148434785" value="-0.000913100392326383"/>
      <parameter name="Scale" free="0" max="1000" min="0.01" scale="1000000" value="1"/>
    </spectrum>
  </source>
</source_library>
```

FIGURE 2.7: XML file of fitting made to Tycho events simulation. ctlike also requires a source mode XML file, at the end of the analysis it returns another XML file in which the parameter values are substituted with the fitting values and their uncertainties (errors). The TS is also shown.

value for the model if no point source exists (the "null hypothesis") M_{-j}.

$$TS = 2\ln M - 2\ln M_{-j} \tag{2.5}$$

$$\text{Where } \ln M = \textstyle\sum_i(-\ln L_i(M))$$

If the number of events (n) is large ($n \to \infty$), the null hypothesis $-2Ln(M_{-j})$ is expected to be asymptotically distributed as χ^2 (chi-square distribution). The integration of the chi-square function from TS to ∞ show that it coincides with the integral of the normal distribution from $\sqrt{TS}$ to ∞. Therefore, this means that a certain position, significance of the events can be defined as $\sqrt{TS}\sigma$ [32]

2.3.3 csspec and ctskymap

The *ctskymap* tool is used to generate a sky map with the events simulated by *ctobssim*. It helps to the visualization of the counts. *csspec* extracts the event simulated and generates a spectrum of flux using ctlike fit tool. It computes the source flux and its statistical uncertainty as well as the significance of source direction. When finish, it creates a FITS file containing a table with the fitted energy and corresponding fluxes and their errors. The number of spectral point can be chosen [7].

Chapter 3

Spectral studies of Tycho, Cassiopeia A and Kepler SNR

We simulated gamma-ray observations at energies between 0.1-200 TeV following different spectral models such as single power-law, broken power-law, and single power law with exponential cut-off. The parameter used on the spectrum were fitted results from measured data. The aim is to prove the ability of CTA to distinguish between the different models and detect possible cut-offs that would prove particle acceleration. Therefore, we also perform a maximum likelihood to estimate the time observation needed to detect different energy cut values. To determine that, single power-laws spectra were fitted using cut-off parameters. Normalization factors and indexes were kept invariant, while the cut-off was changed during the fitting process with E_c values between 2-1000 TeV. Because is not expected to find a cut-off at 1PeV, the log-likelihood for this value (L_{1000}) was assumed as the null hypothesis and the TS was calculated. As it was explained, it is expected that the TS follow approximately the χ^2 distribution and there would be a point where the detection significance equals to $\sqrt{TS}\sigma$.

The case of Kepler SNR it was not possible to find fit parameters due to the lack of gamma ray detection. There exists models based on nonlinear kinetic theory of DSA that predict a possible hadronic spectrum by the analysis the X-ray and radio non-thermal emission. As well, they consider different distances, ISM densities and SN explosion energies to predict different type of spectra. Gamma-ray upper limits were measured by HESS and fitted with one of those models to determine a possible distance and maximum proton or electron energies [27]. The same normalization factor obtained by HESS was used to simulate gamma ray event with a spectrum index Γ of 2.

CTA spectrum simulations were made using an IRF for 50h in the northern hemisphere and assuming 100, 200 and 300 hours of observation. For maximum likelihood

performance, a 50h point source observation at a zenith angle of 20^o were assumed to generate the IRF. Single power-law were simulated for values between 5-100 hours of observation and later fitted with an exponential-cutoff model.

3.1 Tycho SNR

Tycho is a well-studied supernova along with CAS A. Its first observation in 1572 indicates an age younger than 500 years. Light echoes studies of the explosion and X-ray measures of the composition, has classified it as a shell type Ia supernova, and thus a possible candidate for cosmic ray acceleration (Krause et al. [33] and Decourchell, A. et al. 2001 [34] The first reported TeV gamma-ray emission suggested a power-law spectra of $\Gamma = 1.95$. Measures were carried by VERITAS telescope covering a range between 1-10 TeV [35]. Later, Fermi-LAT confirmed high energy rays emitting between 0.3-100 GeV range. The spectrum was described as a power law but with a softer index $\Gamma = 2.3$ (et al. [36]), which it would suggest a possible break. Later results, for both VERITAS and Fermi-LAT measures, shown that the total could be fitted either with a power-law or a power law with a cut- off and it does not appear to show a break in its spectrum. Later results, made with both VERITAS and Fermi-LAT, confirmed that. Results are summarized in table 3.1 [37].

It has been developed different models, all based on the DSA theory, to explain the spectrum of Tycho's gamma ray emission and most of them concluded that it has an hadronic origin, but they differ in the index values (see Slane et al. [38], Berezhko et al. [39], Zhang et al. [40] among others). On the other hand, Atoyan and Dermer [41] modeled leptonic and hadronic emission for Tycho using a two-emission model zone and their conclusion is that both scenarios fit Fermi and VERITAS data.they concluded that the only way to distinguish between both scenarios is to find the pion bump at 100-300 MeV [42].

	Fermi-LAT	VERITAS[35]	VERITAS+Fermi-LAT[37]	
Parameters	Single power-law	Single power-law	Single power-law	Power-law + cut off
$N_0 10^{-13}/cm^{-2}s^{-1}TeV^{-1}$	2.2 ± 0.5	2.2 ± 0.4	1.72 ± 0.29	4.16 ± 2.11
Γ	2.31 ± 0.51	1.95 ± 0.51	2.28 ± 0.03	2.14 ± 0.08
E_{cut}/TeV	–	–	–	1.70 ± 1.23

TABLE 3.1: Fitted parameters obtained for Tycho by VERITAS and Fermi-LAT group between 2008-2014, with their statistical errors

The center of the remnant was measured by Chandra telescope in the X-ray range, and was place at RA 6.34^o and DEC 64.13^o (et al. [43]). The first VERITAS observations suggested a point source TeV gamma-ray emission, but with a peak that seem not to coincide with the center of Tycho [37]. This misplacement does not seem to be very

significant, but is enough to question if the gamma-ray emission is due to a molecular cloud rather than coming for the shell. HI and CO measures (Reynoso et al. [44], Lee et al. [45]) suggested that this could be possible. Centroid measures and modelings made by Archambault et al. 2017 [46] concluded a TeV gamma emissions coming from the center of the remnant. Also, they analyzed the type of the source concluding that a point source and a shell source are the most probable scenarios , with a highest significance of the first over the second.

3.1.1 Results

CTA simulations were made using table 2.1 parameters for 100, 200 and 300 hours observation assuming a point source emission.Simulations were made using a power law, a broken power-law and power law with a cut-off. We simulate events for each of the models assuming an IRF for the northern hemisphere and generated for 50h observation. The simulated events have an energy range between 0.1 and 200 TeV. Events distributions and fitting results are shown in table and figures below.

The TS value compares the log-likelihood value of the model with the log-likelihood of the same model if no point source exists. Statistically, the best results would be those which maximize the log-likelihood function because it would mean that the assumption of no source is incorrect. Therefore, different observations of the same model with the same null hypothesis and the best data fit will correspond to the one with the larger log-likelihood value. If we assumed that the square root of the TS was approximately equal to the detection significance of the source, the best fit spectral parameters would have been those that had the lowest TS compare to other models. In the case of Tycho, best fitting spectral analysis are obtained for more hours of observation, and the exponential cut-off and single model used are favored over the rest for more than 100h of observation with similar statistical relevance.

Model	TS(100h)	TS(200h)	TS(300h)
Broken	3297	6056	10076
Single	1238	2909	3605
Cut-off	1246	2224	3605

TABLE 3.2: Test statistical values obtained during the fitting analysis of the generated events of Tycho SNR

The skymaps represent the event generated in the different simulations. The distribution of the generated events are concentrated in the remnant center as it was simulated, the rest are probable result of CTA detection performance that the software label as background. The IRF includes templates of the background distribution that can be

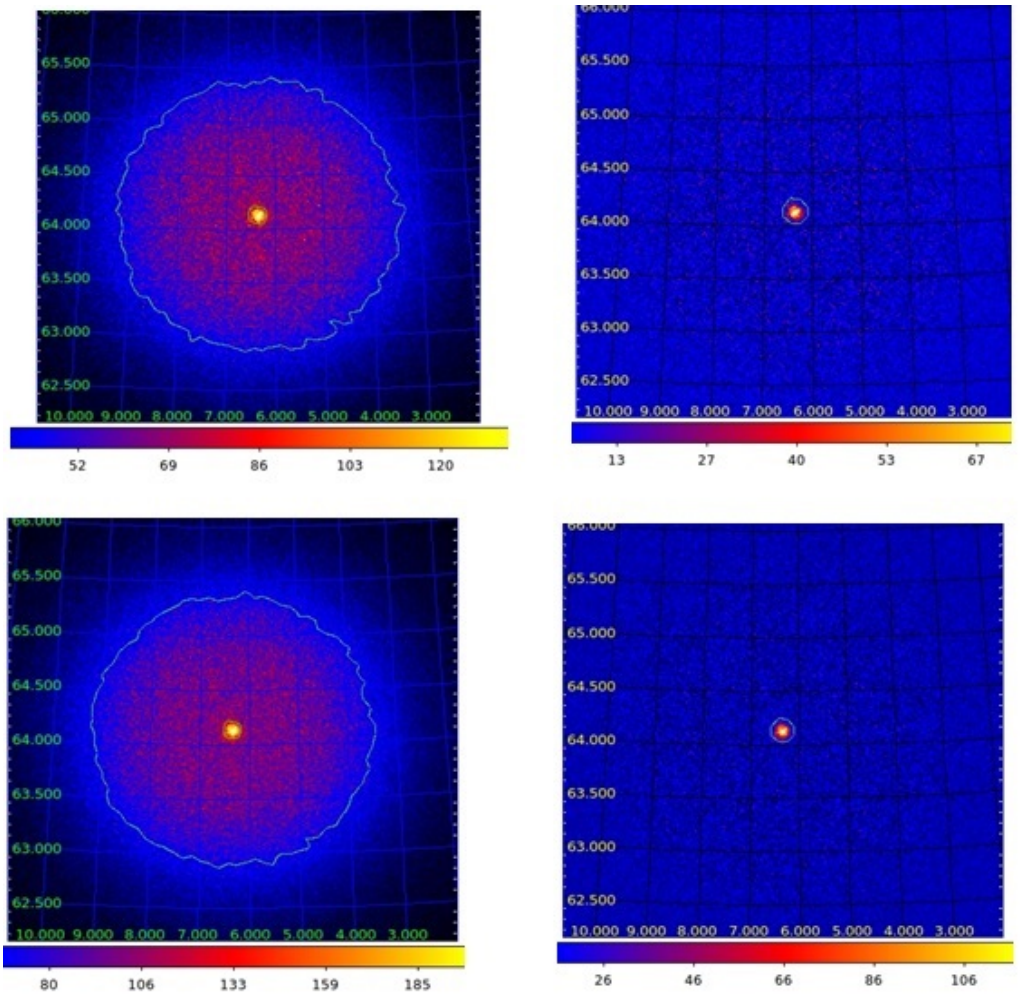

FIGURE 3.1: Sky map obtained for 100, 200, 300 hours of observations (top to bottom respectively). In the left side, it shows the sky map of Tycho centered at RA 6.34^o and DEC 64.13^o (remnant center) in celestial coordinates for the energy range between 0.1-200 TeV. On the right, the same sky map with background subtraction. The green contours combine all the events generated showing a maximum in the center. Images were generated using the broken power-law model.

used to eliminate those events that difficult the source recognition, in figure 3.1 it shows the skymap events of the broken power-law with and without background subtraction. Nevertheless, because non background subtraction model was considered, the different skymaps obtained confirmed that for Tycho CTA would need more hours observation not only to distinguish between models but also to detect possible gamma-ray emission of the center of the remnant and avoid other possible sources or background contamination.

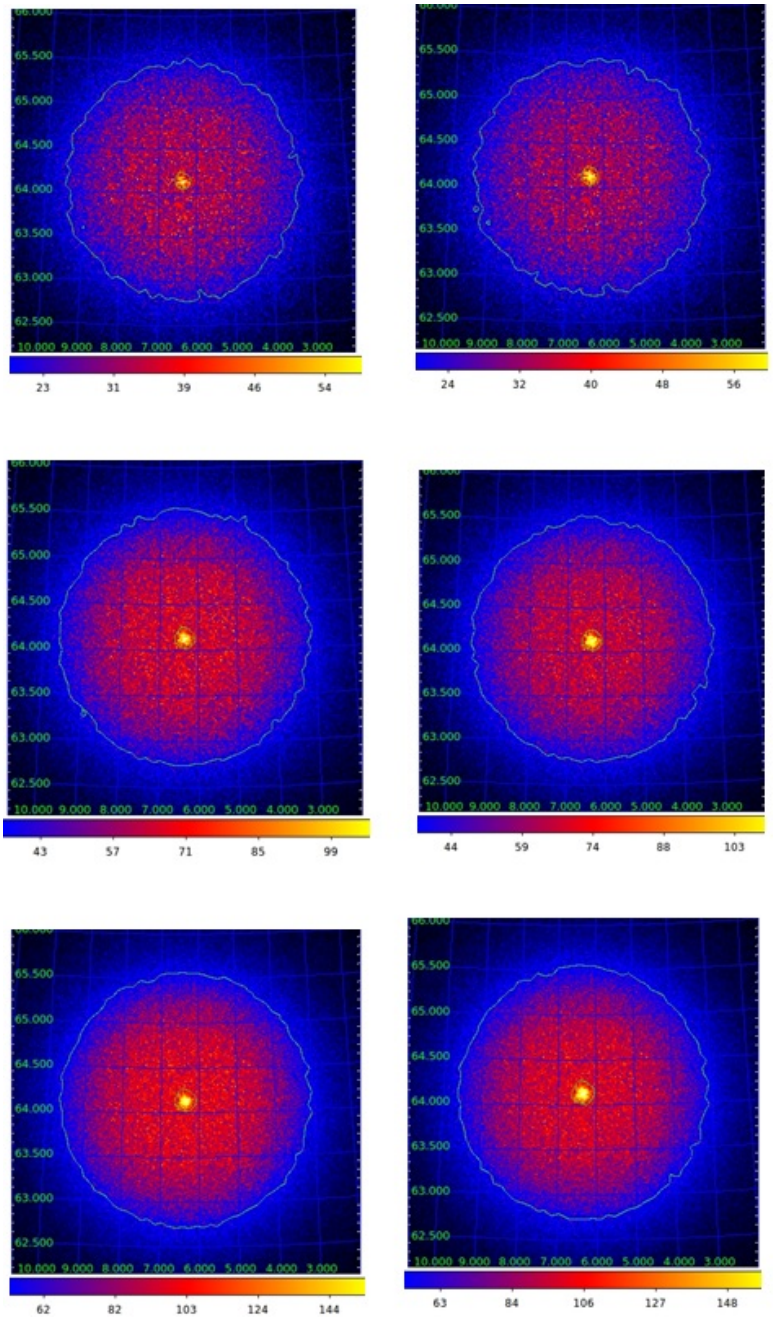

FIGURE 3.2: Sky map obtained for 100, 200, 300 hours of observations (top to bottom respectively). It shows the sky map of Tycho centered at RA 6.34^o and DEC 64.13^o (remnant center) in celestial coordinates for the energy range between 0.1-200 TeV. On the right, the sky map corresponds to single power-law mode.Pictures on the left correspond to single+cut off power models. The green contours combine all the events generated showing a maximum event in the center.

3.1.2 Spectral analysis

We simulated a photon spectrum for 100, 200 and 300 hours with the parameters listed in table 3.1 to analyze the ability of CTA to distinguish between the different spectra proposed for gamma-ray Tycho emission. This would allow to distinguish between different acceleration theories and/or improve them. In the case of Tycho, the obtained different spectrums show similar normalization factors and indexes, that only can be clearly differentiate at higher energies. This can clearly be seen on the simulated photon spectrums for different observation times. The difference between two power-law models becomes to be clear for values over 10TeV. Because of that, distinguish a possible break around 1TeV would be hard.

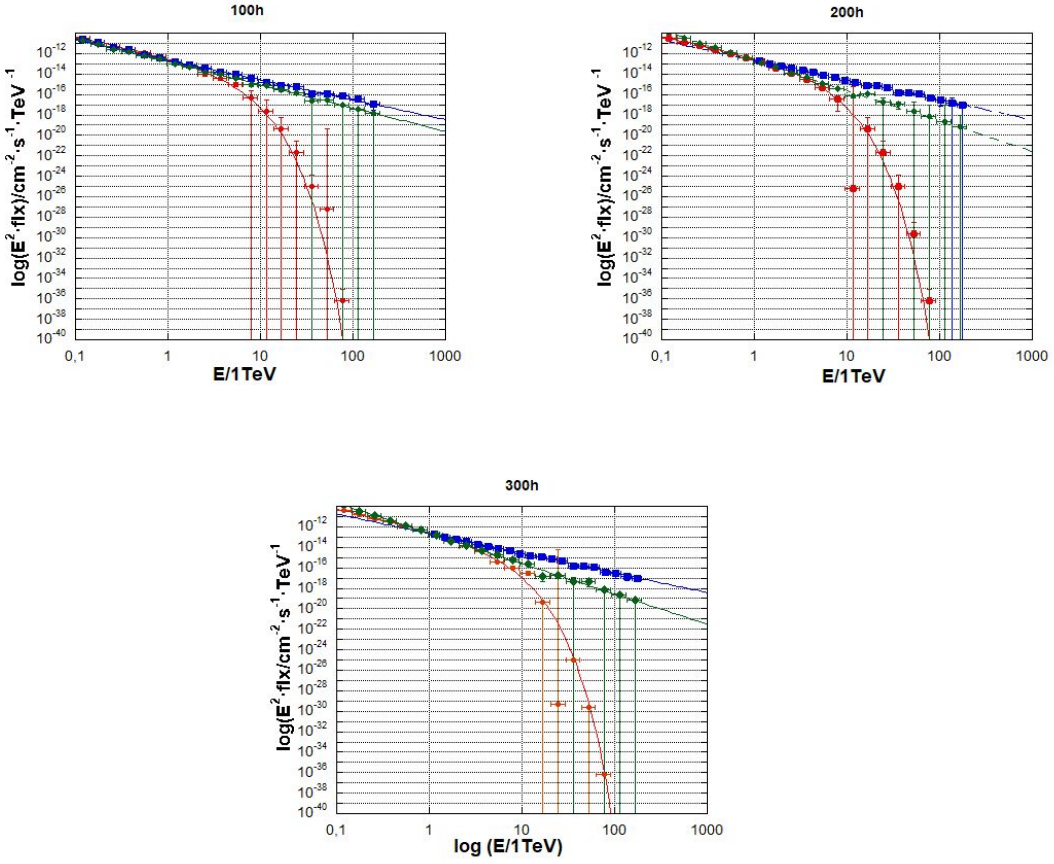

FIGURE 3.3: Simulated spectrum of Tycho for 100, 200 and 300 hours CTA observation and assuming 20 events. Blue and green spectrum correspond to the broken power-law model and single power-law respectively. Red spectrum corresponds to a single law with exponential cut-off

However, the used broken power-law scenario seems the less probable for Tycho gamma-ray emission, based on the TS analysis made. The best fitting corresponds to a spectrum with a cut-off, which CTA will be able to distinguish clearly for values

$>$ 5 TeV between the other power-law spectra. The exponential cut-off model used, predicted a cut-off on 1.7 TeV, but it is possible that in the future appears variation on that spectrum if we assumed that the maximum CR energy depends on the SNR age. As it was said, cut-off detection is important to probe particle acceleration. Therefore, we also analyzed the ability of CTA to detect a possible cut-off in the $\Gamma = 2.28$ power spectrum. The obtained single power-law by Archambault et al. 2017 [46] was simulated using a 50h point source observation at a zenith angle of 20^o as the IRF.

Later a maximum likelihood analysis was made using an exponential cut-off model, varying the energy cut (E_{cut}) between 2-1000. Assuming a detection significance of 2σ as acceptable for the different energy cuts, the results shows that CTA would detect cuts up to 54 TeV. For that spectrum, the E_{cut} detection seems to decrease for observation times greater than 75h and does not seem possible to detect cut energies around 100 TeV.

Time/h	5	25	50	75	100
E_{cut}/TeV	5.27	10.44	48.6	54.3	41.1

TABLE 3.3: Energy cut values corresponded to $\sqrt{TS}\sigma = 2\sigma$. Only rough estimation is considered

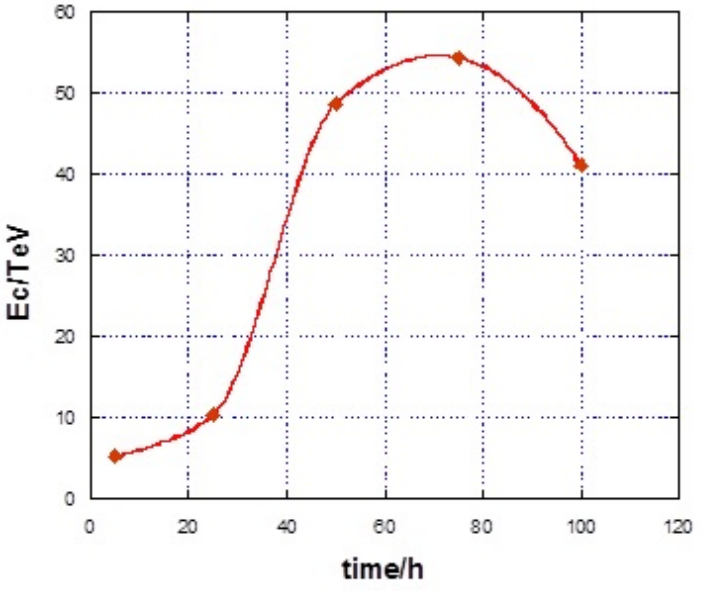

FIGURE 3.4: Representation of cut-off energies obtained on the maximum likelihood analysis for possible cut-off detection for 2σ detection significance.

3.2 Cassiopeia A SNR

Cassiopeia A or Cas A is a shell-type supernova which center has been located at RA(J2000) 350.83^o and DEC (J2000) 58.82^o by X-ray measures (et al. [47]). Based on light echoes observations, it was defined as Type IIb explosion (Krause et al. [33]) located at ~ 3.4 kpc (Reed et al. [48]) and aged 400 years or less.

The first gamma ray emission was reported by HEGRA [49] and MAGIC telescope [49] at the TeV regime. They measured a spectra consisted in a single-power law with indexes $\Gamma \sim 2.5$. Later, Fermi-LAT detected gamma-ray emission at GeV with photon index $\Gamma \sim 2$ suggesting a possible break in power-law spectrum (Abdo et al. [50]). Measures made by VERITAS between 0.3 and 7 TeV report a single power-law emission with $\Gamma \sim 2.75$, with no sign of break in the spectrum [46]. But analysis made combing differrent Fermi-Lat and VERITAS measures [51] seem to be favored for a break power-law spectrum. This break would be located at 0.2 TeV which is in lower than VERITAS energy range. SHALON observations reported a possible exponential cut-off spectrum for Cas A. Although, the significance is much higher (16σ) than the other spectrum proposes[52].

The origin of the gamma-ray emission from Cassiopeia seems to have an hadronic origin, but also a leptonic emission cannot be excluded. Infrared observations (Wallström et al. [53]) reveled ro-vibrational and high-J rotational CO lines coincident with the reverse shock. This could suggest a possible interaction with a molecular cloud, but no significant evidence has been found that associates the TeV emission with the molecular cloud interaction (Kilpatrick et al. [54]). X-ray measures reported a compact object close to the center of the remnant (Pavlov et al. [55]), however does not seem capable enough to generate detectable gamma-ray (Abdo et al. [50]). Also X-ray and radio observations shown forward and reverse shock that would suggest that the remnant is expanding into the ISM and producing Thermal and non-thermal emission inside the shock. Chandra observations reported a different magnetic strength values inside the shock. In the northwestern part higher values were found in contrast with the south, which means that inverse Compton is less significant in the north than in the south, due to higher value of the magnetic field.

Analysis made using VERITAS, Fermi-LAT and MAGIC data suggested that at least at lower energies, leptonic scenario predicts less flux that what is observed. At TeV range both hadronic and leptonic model seem favored over a single hadronic or leptonic emission. The limited angular resolution of telescopes difficults to differentiate the contribution of leptonic or hadronic to the gamma-ray emission of the shock. The angular dimension of the radio and X-ray emission coincides with the angular resolution

of VERITAS and MAGIC telescope (0.08^o) over 1TeV. For GeV energies, the resolution is better (0.06^o) which allows a better distinction between different possible scenarios.

	VERITAS(Kumar 2015)	VERITAS+Fermi-LAT(Ghiotto 2016)	SHALON(Sinitsyna and Sinitsyna 2016)
Parameters	Single power-law	Broken power-law	Power-law + cut off
$N_0 10^{-12}/cm^{-2}s^{-1}TeV^{-1}$	1.45 ± 0.11	0.7 ± 0.1	0.64 ± 0.10
Γ_1	2.75 ± 0.10	2.10 ± 0.04	0.91 ± 0.11
Γ_2	–	2.78 ± 0.10	–
E_{break}/TeV	–	0.220 ± 0.78	–
E_{cut}/TeV	–	–	10.3 ± 1.2

TABLE 3.4: Fitted spectral features and values obtained by VERITAS, Fermi-LAT and Shalon telescopes of Cas A gamma ray observation

3.2.1 Results

As in the previous case, CAS A spectrum was simulated in the 0.1-200 TeV range for 100, 200 and 300h. We simulated single-law, broken power-law, and single power-law with a cut- off using VERITAS, Fermi-Lat and SHALON obtained parameter spectrums listed in Table 3.4.

Initially likelihood analysis showed very high values of TS, indicating that less hours of observation will be sufficient to distinct between the different spectra models. Results show that the best fitting results are obtained with the exponential cut-off model. TS values for the broken power-law are too low that the null hypothesis cannot be excluded. The explanation could be that the break around 0.2 TeV it is too low to be detected by CTA. Comparing Fermi-LAT and VERITAS measured data with the simulated photons spectrum, seems to confirm the broken power-law spectra over the single power-law. The possible break would be detected clearly if the energy rage is extended below 0.1 TeV.

Model	TS(25h)	TS(50h)	TS(100h)	TS(200h)	TS(300h)
Single	8216	17491	33764	67159	101764
Cut-off	8032	16411	32916	66610	97752
Broken	16	21	47	69	110

TABLE 3.5: Test statistical results obtained during the fitting analysis of the different models generated events of CAS A SNR

The same way as Tycho, no background model was considered for the event simulation. The skymap representation of the events of Cas A does not show as much as wide-spread as can be seem in Tycho analysis. Therefore, few hours of observation would be enough to detect a possible emission coming from the remnant center.

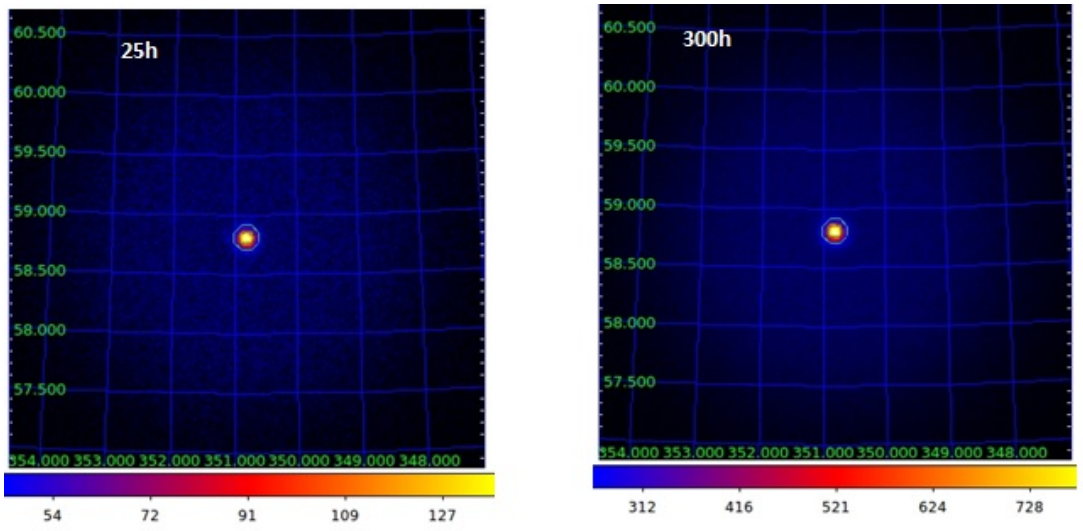

FIGURE 3.5: Simulated single power-law sky map obtained for 25 and 300 hours of observations of Cassiopeia. Mayority of the events are centered at RA 350.81^o and DEC 58.80^o (remnant center) in celestial coordinates for the energy range between 0.1-200 TeV. The green contours combine all the events generated.

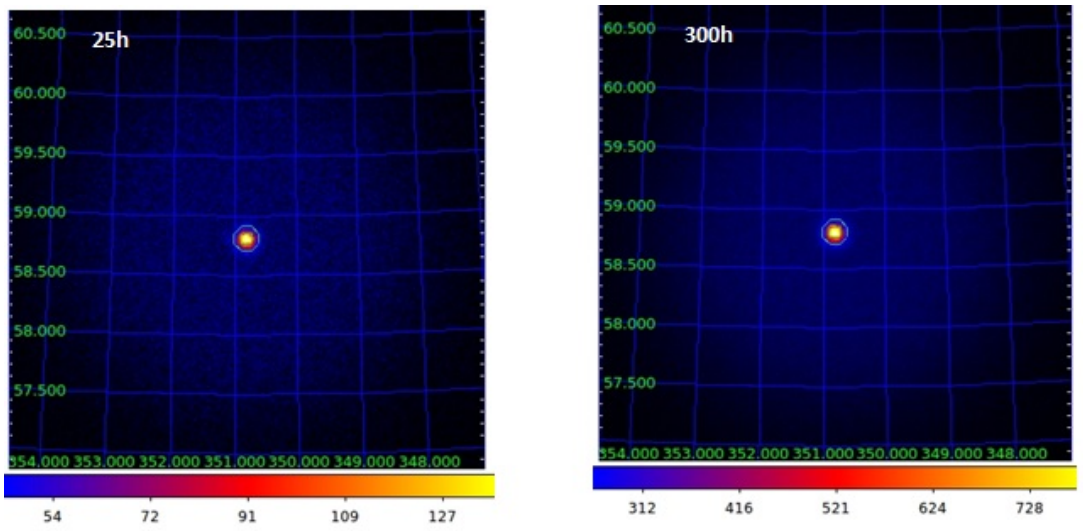

FIGURE 3.6: Simulated power-law+cutoff sky map obtained for 25 and 300 hours of observations of Cassiopeia. The events are centered at RA 350.81^o and DEC 58.80^o (remnant center) in celestial coordinates for the energy range between 0.1-200 TeV. The green contours combine all the events generated showing a maximum grouped in the center.

The exponential cut-off spectra obtained by SHALON telescope goes up to 30 TeV while VERITAS goes up to 10 TeV. A combination of the 3 possible model spectra (single, broken, and exponential cut-off) could explain the spectra measured by SHALON telescope and it would be suggesting a possible presence of a cut-off in the VERITA power-law photon spectrum. Therefore, the same way as done for Tycho, simulation of the single power-law was made for 5-200 hours of observation with a generated IRF with 50h and 20^o fixed zenith angle was made. Later, the results where fitted with an exponential cut-off model with different energy cuts.

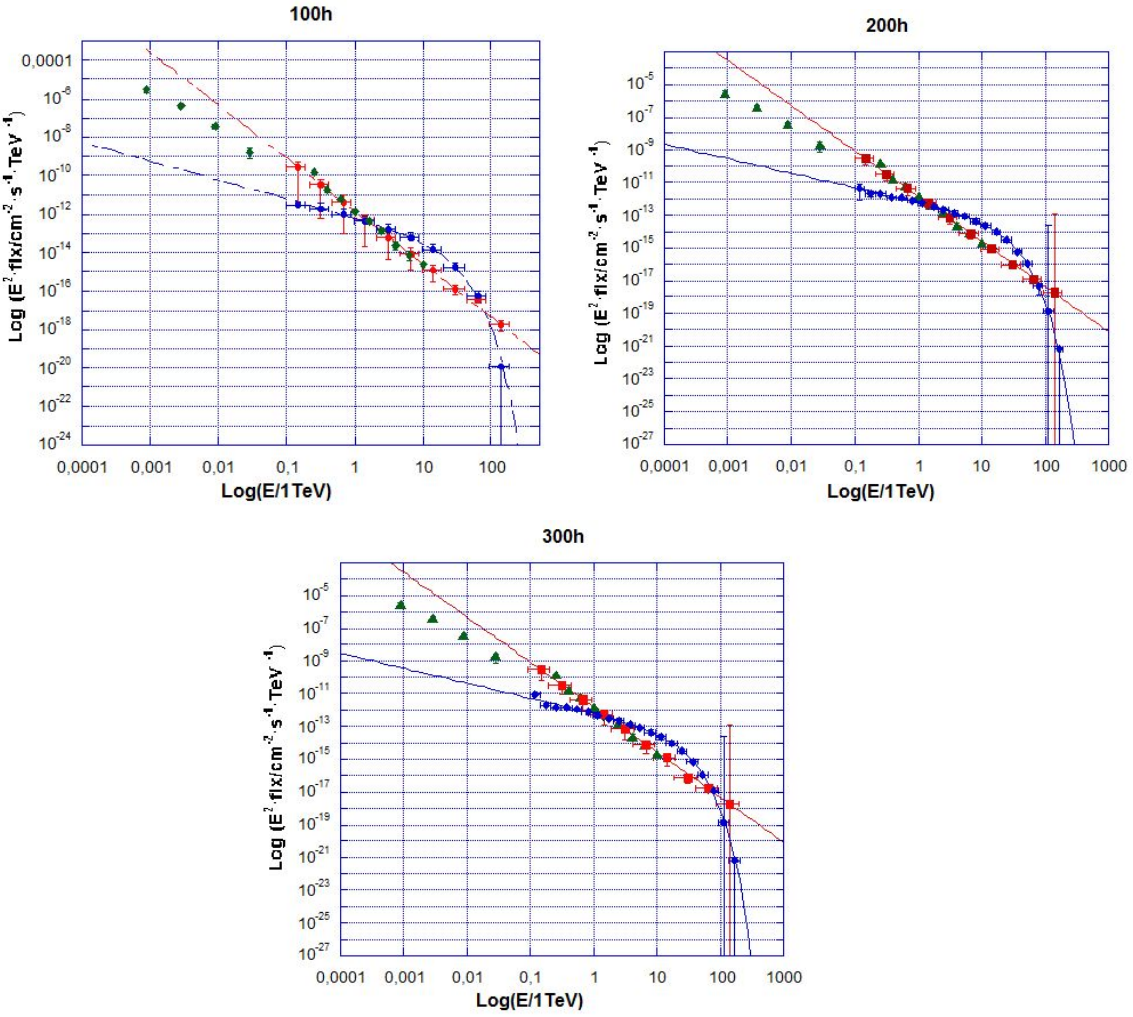

FIGURE 3.7: Representation of real and simulated photon spectrum data for Cas A. The red and blue spectra corresponds to the single and the exponetial cut-off models simulated. Green data corresponds to data measured by Fermi-LAT and VERITAS.

In this case, we considered a detection significance of 3σ as best fit for the cut-off energy. As well as seen in Tycho, for 100h observation an increase of energy value implies a reduction on the detection significance. Probably, this would be a consequence of Wilk's theorem violation and the rough estimation that have been taken. Results

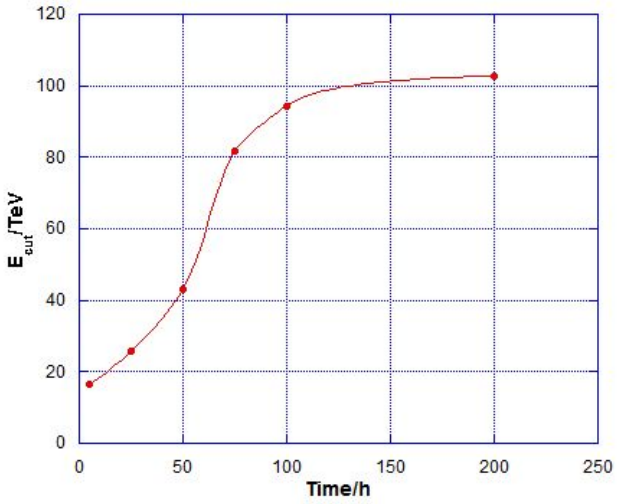

FIGURE 3.8: Representation of Energy cuts obtained in the likelihood analysis performed for Cas A. For 100h observation the Energy with 2σ is represented.

showed that CTA will be able to detect a possible 100 TeV cut-off energy in the power-law. But to achieved that, at least 200 hours observation of Cas A would be needed. For Tycho, a 200h observation with that IRF was not able to be performed due to the large computational time needed. However, if the same amount of time employed by VERITAS on Tycho observation ($\sim 150h$[37]) were used for Cas A, CTA would detect a possible cut around 100 TeV. In conclusion, Cassiopeia seem to be a better candidate than Tycho to measure CR ray acceleration.

Time/h	5	25	50	75	100	200
E_{cut}/TeV	16.7	25.7	43.05	81.94	72.91/94.3(2σ)	102.8

TABLE 3.6: Energy cut values corresponded to $\sqrt{TS}\sigma = 3\sigma$ for Cas A likelihood analysis. Only rough estimation is considered.

3.3 Kepler SNR

Kepler supernova located at RA(J2000) 262.68^o and DEC(J2000) -21.52^o, also seem to be a very good candidate for searching cosmic ray because of it age ($\sim 440 years$) and type. Fermi-LAT first catalog reported a GeV emission from Kepler with $\Gamma = 2.3$ (Acero et al. [56]), but nothing in the TeV regime. CTA performance, its location, a possible presence of an ISM with different density and type of explosions complicates the detection and analysis of gamma ray spectrum.

Measures made using historical light curves (Baade [57]) suggested a type Ia supernova, corroborated by later X-ray studies on O/Fe ratios (Reynolds et al. [58]). It has been argued a possible type II origin of the remnant, based on interpretations of light curves (Doggett and Branch [59]) and evidences of a circumstellar shell medium (CSM) that is interacting with the remnant (Vink [60]) but newer studies base on XMM-Newton, Chandra, and Suzaku observations suggested that it would have been expelled years before the explosion and now it is showing possible proves of interaction (Katsuda et al. [61]). Same X-ray spectrum, seem to confirm the type Ia supernova base on the presence of Fe and Fe groups spectral lines (Katsuda et al. [61], et al. [62]). XMM-Newton confirmed high abundance of nitrogen and silicates in the remnant, which would indicate a progenitor star with masses around $4 - 6M_{\odot}$ and therefore the energy of the explosion would be less than the typically 10^{51} erg.

HI absortion studies made by Reynoso et al. [44] conclude an upper and lower limit of the distance between 4.8-7kpc. Sankrit et al. [63] argued a value of 3.9 kpc measuring the motion of optical filaments, Vink [60] studying the SNR forward shock suggested a distance greater than 6kpc or $\sim 6kpc$ if the explosion was sub-energetic. New measures of light curve made by Ruiz-Lapuente [64]) suggested a possible distance of 5 kpc, same as revise results of the filament motion (et al. [65]). Their results are consisted with the BKV prediction of Kepler gamma-ray spectrum. The BKV theory is a revised non-linear DSA theory introducing the magnetic amplification due to plasma instabilities. Measures made in the KeV band shown possible shock acceleration of electrons from 10-100TeV. Narrow filaments were found in the outer region of the SNR, thought to correspond to X-ray synchrotron emission. In the northwestern part, there is also evidence of thermal bremsstrahlung emission (et al. [66]). HESS measures concluded that an inverse Compton scattering gamma-ray flux will produce lower upper limits than the measured ones.

Measures at radio and X-ray band also shown that the northwestern part is expanding faster with a lower rate than the southwestern part. This would indicate that the surrounding is inhomogeneous. The spectral BKV model assumed a spherical symmetry, average expansion velocity for the remnant and different average densities for the ISM. In conclusion, the results obtained by HESS, seem to be consisted with the estimation made by Berezhko et al. (2006) [67] for a distance of at least 6.4 kpc, density $n = 0.7cm^{-3}$, energy explosion of $\sim 10^{51}$ erg and eject mass of $1.4M_{\odot}$. Even though, the evidence of high densities and nitrogen-rich materials suggest a significant mass loss of $\sim 1M_{\odot}$.

3.3.1 Results and Analysis

We considered the upperlimits parameters detected by HESS [27], which seem to coincide with the expected spectrum of Kepler obtained by non-linear kinetic model for $d = 6.4$ kpc and density $n = 0.7cm^{-3}$. Their analysis also concluded an hadronic scenario for the emission detected, which implies a possible spectrum with index ~ 2. Using those parameters, a single power-law and exponential cut-off was simulated for 25, 50 and 100 hours of observation with index $\Gamma = 2$ and $E_{cut} = 100$ TeV. BKV theory also predicts a possible spectrum for 7 kpc and $n = 0.7cm^{-3}$ [67], because HESS upperlimits suggest a distance greater that 6kpc also that spectra was considered and models with the same conditions.

Distance/kpc	Density/cm^{-3}	$N_0 \dot{1}0^{-13}/ergcm^{-2}s^{-1}$	$N_0 10^{-13}/cm^{-2}s^{-1}TeV^{-1}$
6.4	0.7	3.4	4.017
7	0.4	1.6	1.926

TABLE 3.7: Integrated flux values obtained by HESS for distance of 6.4 and 7 kpc and corresponding densities values. The gamma-ray flux was measured between 0.23-12 TeV and seems to correspond to 6.4 kpc.

The different simulated models shows that an exponential cut-off model is preferred over the single power-law. However, better fitted results are obtained for 7 kpc rather than 6.4 kpc, consisted with the results obtained by CANGAROO and HESS telescope. Simulation performance of CTA from the analysis of different SNRs concluded that for type Ia, emission spectrum would be detected up to 5kpc or 10 kpc if the source has around 1000 years old[25]. This will mean that for distance greater than 6 kpc, it would be necessary to wait a couple hundred years to obtained a clear gamma-ray spectrum. The different DSA models explained that the maximum energy of CRs confined in the shell depends on the SNR. With age, the shock velocity decays and, also, the downstream magnetic field strengthen around the shock. The SNR capability to confine particles is reduced as well and particles are scattered with less maximum energy. Energy cut evolution could be considered that approximately decays linearly with time, following the expression:

$$E_{cut} \sim t^{-\alpha} \tag{3.1}$$

Where t is time of the remnant and α is CR source parameter and is generally assumed with a value of 2.6

If, at this moment, Kepler has an age of 413 years, approximately the evolution rate for this SNR would be:

$$\frac{dE_{cut}}{E_{cut}} \sim -\frac{\alpha t^{-\alpha-1}}{t^{-\alpha}} = -\frac{\alpha}{t} = -0.006yrs^{-1} \tag{3.2}$$

d=6.4 kpc		
Model	*time*/*h*	TS
Exponential	25	28540
	50	59155
	100	116742
Single	25	31730
	50	65028
	100	125437
d=7 kpc		
Model	*time*/*h*	TS
Exponential	25	11504
	50	23287
	100	46231
Single	25	12074
	50	25980
	100	51003

TABLE 3.8: TS Results obtained by ctlike maximum likelihood analysis made for Kepler, for distance of 6.4 kpc and 7 kpc

This implies that in a period of 200 years, E_{cut} would have decrease 120% of its actual value [15]. Even though this is a rough approximation, it shows the possibility of no cut-off detections in the future.

Chapter 4

Results and Discussion

We addressed the potential of CTA on the study of TeV emission SNRs. The aim is to detect proves of particle acceleration and spectral features that link SNRs as Cosmic-ray sources. Different DSA theories explain the CR ray acceleration inside the remnant, but implies certain constrains such as type, age, energies,etc. that reduce significatively the number of supernovas that participate in the CR injection.

It was believed that the confined of particles in the center remnant provides the sufficient acceleration to the PeV range. However, detection of other TeV sources such as pulsar wind nebulae (PWN), molecular clouds near SNR, composite SNR, galaxy center, etc. opened the door to other mechanism of CRs acceleration. In the case of shell type SNR, it is expected a very large shock velocity and large magnetic fields due to plasma instabilities, during the free expansion phase [16]. However, the duration of this "PeVatron phase" seems to last less than 100 years [23]. Studies of CTA performance suggest that spectral and morphology features of young SNR ($< 1000 yrs$) would not be easily measured at least there are very close and are surrounded by a homogeneous ISM [25]. Therefore, recent SNR detection such as G1.9+0.3 (~ 110) and in the outer galaxy such as SN1885, SN1895 and SN1937C cannot be considered. Even though, that is believed that CR spectrum up to the knee have an unique source within the galaxy.

So far, Tycho and Cas A have been proven the best sources of gamma-ray emission for purposes of spectral studies. They have been very well studied by different satellite telescopes and IACTs, we analyzed how the future improvement of Cherenkov telescopes will affect in the observable spectra of Tycho and Cas A. Their age is clearly larger than 100 years so a PeV detection is not expected. However, because the evolution of the remnant causes at least 10% decay in the spectrum in form of a cut-off, a spectral decay around 100 TeV will prove that there was an acceleration up to 1 PeV in the past. In the case on Tycho, the improvement in the energy detection will help to distinguish

clearly between the different model propose for the gamma-ray spectrum. Our results show, that the best fit is obtained with the exponential cut-off model, followed by the single power-law. The cut-off calculated by VERITAS is around 1.7 TeV [37], much lower that it would be desired. If the power-law spectra is assumed, a possible 100 TeV cut-off detection is not very clear. Much more observation hours than those performed by VERITAS, seem to be needed to detect a possible cut-off and to modeled a better gamma-ray spectrum, at least 300h base on the maximum likelihood results. On the other hand, Cassiopeia results show that to obtained a clear spectrum not so much observation hours are needed. In this case, broken power-law is prefered over the single one. The break in the energy is in the lowest detection regime of the future CTA (~ 0.2 TeV). The detection of that possible break would be in a combination analysis with GeV data obtained with another telescopes. Studies made of Cas A and Tycho, combining Fermi-LAT and VERITAS data, showed better spectral results. Results of Cassiopeia also show, that a possible cut-off of 100 TeV could be detected if around 200h observation it is perform. The improve of angular resolution and possible cut-off detection make Cas A a good candidate for CTA observation.

The case of Kepler SNR, the large distance prevents a clear detection of gamma-ray emission. As it was said in section 3.3, the upperlimits measured by HESS and CANGAROO suggested a distance larger than 6.4 kpc [27], [68]. The better likelihood analysis performed using the BKV parameters suggest that better fit is performed with the 7kpc values. This, joined to the fact that seems to be in a non-homogeneous environment, would not possible be clearly detected until it reaches 800-1000 years, at least with CTA. Therefore, it does not seem to be as good candidate to gamma-ray spectra measurement as it could have been thought. The relativistic accelerated protons responsible of CRs, produce a cascade of secondary particles which some of them are expected to produce gamma-ray also in the GeV/MeV regime. The detection X-ray and radio synchrotron emission due to electron production in the interactions, along with the gamma-ray detection at low energies, would carry information about the possible acceleration in the remnant. Kepler have been measured clearly in the X-ray and Radio regime and shows possible synchrotron emission in the outer part of the remnant and probable future measures show gamma-ray emission in the MeV/GeV. However still no evidence has been found yet that link this with the PeV emission, but that could change in the future.

4.1 Possible PeVatron sources

Gamma-ray detection of SNR could be explain by interaction of relativistic particles, but still it cannot take this as a prove of remnant contribution to the CR bulk. The

amount of CR reaching the earth require a constant injection of particles, during a periods greater than 10^3 years. Base on spectra models and CTA capabilities, the detection of young SNR that are accelerating particles have a lot of constrains. It would require a very young SNR ($< 100 year$), very close and that could be measured during a great period of time to characterize its spectral evolution. At this moment, not such remnant has been detected. Recently HESS collaboration reported traces of PeVatron in the inner parts of the galaxy. This region has a greater rate of star formation with higher probability of founding younger supernova explosions. However, the injection problem still remains. The shocks speed seem to be not enough and not last enough to accelerate particles to the reported energy. The reported gamma-ray is located in a radius of ~ 10 pc in the inner galaxy, coincident with HESS angular resolution. In this radius also other possible cosmic ray sources can be considered.

Stellar clusters are groups of thousand or even millions of stars packed in small regions of $\sim 1 pc$ [15]. Near the galactic center, there exist very high population of stellar cluster that have been reported in the GeV/TeV regime or show thermal and non-thermal emission. This are the cases of Arches and Quintuplet cluster. XMM-Newton proved thermal emission due to multiple star wind collisions (Capelli et al. [69]). Chandra observations suggested that non-thermal emission could have been produced by interaction of low energy CR electrons with a dense molecular cloud (Wang et al. [70]). However, none of this clusters seem to show gamma emission and seem to be located outside of the possible PeV accelerator area.

The supernova explosions in this high density group of stars could lead, along with the stellar winds, to the ne magnetic turbulence necessary to provoke magnetic amplifications that accelerate particles. There exist proves of molecular cloud near some clusters that have reported Gev/TeV emission, such as the Westerlund 1 and 2 massive star cluster (Asahina et al. [71]). In young stellar clusters, models predictions of acceleration efficiencies and possible spectra show that some of stellar clusters that emit gamma-ray emission, 10% or even less of the stellar wind would be converted into acceleration of particles. For older clusters, the efficiency could be better due to the high amount of stellar wind and supernova events. Also, models show that CTA will be able to detect stellar cluster with conversion efficiency higher than 1% [72]. On the other hand, the amount of massive stars near the center seem not to be enough to generate enough stellar winds and supernova explosions to accelerate particles up to PeV energies. Within the $\sim 10 pc$ radius, VHE TeV emission has been reported from Terzan 5 globular cluster. It is expected that globular cluster might emit leptonic gamma-ray emission due to the large amount of stellar wind collisions and its high amount of pulsar wind nebulae (PWN). However, the reported TeV emission seem not to fit either the hadronic or leptonic scenario (H.E.S.S. Collaboration et al. [73]).

Surrounding the center of the galaxy, also a group of high density molecular clouds are located. The gamma-ray emission reported by HESS collaboration is also in the angular resolution of the central molecular cloud, as they are called. Gamma-ray emission has been reported coming from the same place that the possible PeVatron source. This source show a clear spectrum correspond to leptonic emission, that are as results of relativistic electrons [74]. This could be explain by a possible X-ray pulsar detected by Chandra and NuStar (HESS J1745-290). This object has a harder photon spectrum with a clear cut-off (et al. [75]). It is not very clear that an actual PWN is responsible of that emission and the hadronic scenario seem to be also plausible. The spectrum reported by HESS collaboration et al. (2016)[15] does not show any cut-offs, so another mechanism should be introduce to explain both fluxes. One explanation is the presence of a proton accelerator inside the 10pc region, that in the past could have been ejecting protons up to PeV that have propagated through the outer parts of the molecular clouds which now are emitting gamma-ray emission due to collisions. Because the acceleration efficiency decrease with time, the inner parts of the cloud region is developing cut-off on the spectrum. This cut-offs seem to be decreasing towards the galactic center [76]. The accelerator could belong to an active past of the supermassive black hole. The improve of CTA angular resolution to around 0.02^o for energies greater than 10 TeV , could help to reduce emission area and distinguish between different scenarios (et al. [77]).

Chapter 5

Conclusion

Different DSA theories explain the CR ray acceleration inside the remnant, but they imply certain constrains such as type, age, energy, etc. that reduce significantly the number of supernovas that participate in the CR injection. At the end, we present Tycho, Cas A and Kepler SNR as better candidates to find CR ray acceleration base on CTA constrains and focusing in the northern hemisphere location.

In chapter 2, it is describe the different tools existed and used to observed, treat and simulate gamma ray emission. It is explain also GammaLib and Ctools which are the software used for data analysis in this work.

In chapter 3, it is presented the analysis and results obtained with gamma ray simulation of the chosen SNR . The aim was to address the potential of CTA to distinguish between the most common gamma ray spectral models (Single-law, Single-law with and exponential cut-off and broken power law) and in the detection of possible cut-off in the single spectrum that would prove particle acceleration. To do so, maximum likelihood methods were made to estimate the time observation needed for CTA to detect those possible cut-offs.

Assuming point source emission and an IRF obtained with 50h observation at 20[a]-zenith angle in the northern hemisphere, we obtained the following results:

Tycho SNR case:

The gamma ray simulation shows that single power and single power with a cut-off as the most favoured models for Tycho SNR spectrum. The significance between those simulation is not much (see 3.2), but it is clear that and increase in the energy range detection would help to distinguish more clearly between both models. CTA clearly would detect cut-off grater that 5 TeV, however, no difference in the spectrum appeared if the time observation is increase(see 3.3).

The maximum likelihood analysis showed that CTA would possible detect a a maximum cut-off at aprox. 54 TeV in the linear spectrum with 75h of observation and 2σ detection significance (see 3.3 and 3.4).

Cas A SNR case:

As well as happened with Tycho, an increase in the energy range would better diferenciate between models and no dofference is seen if the observation time is increase $>$ 100 h. The better fit results correspond to the broken power-law specta 3.5. To detect a possible broken-power law spectrum, CTA would detect clearly energy breaks lower than 0.1 TeV (see **??**). For a detection significance of 3σ, the maximum likehood analysis showed a possible cut-off detection in the linear spectrum with 200h observation. Therefore, this case seem a better candidate for measure CR acceleration. (see 3.2.1 and 3.8)

Kepler SNR case:

The analysis of Kepler spectrum results to be a worst candidate that it was thougth that it could be. There is a leak of gamma-ray detection due to its location and sourronuding medium. The BKV model data prediction were used, which seem to be consistent with the upperlimits measured by HESS telescope (see 3.7). Those values showed a better fit for a distance of 7kpc rather than 6.4 kpc with an exponential cut-off model prefer over the single power law (see 3.8). For type Ia supernova, CTA performance analysis showed a detection in the 5-10kpc if the source has around 1000 years old. If , at this moment, Kepler gamma-ray spectrum has a cut-off of a $>$ 100 TeV, cut-off would not possible being seen in the future (see equation 3.2).

In conclusion, the new CTA will help to clarify between the different gamma-ray spectra and would allow the studies of another sources which seem better candidate of CR detection over 10^{15}. It is believed that young SNR contribute somehow to the general CR spectra but because of results and constrains named in chapter 1 and 4, would be hard to find proves of acceleration up to 100 TeV on SNR. Therefore, also in chapter 4.1 we propose another TeV emission objects that are being studied. The future seem to be at Sagittarius A* (center galaxy), where recent HESS observations detected a possible 1 PeV particle.

Bibliography

[1] T.K. Gaisser. *Cosmic Rays and Particle Physics*. Cambridge University Press, 2004. ISBN 9780521016469.

[2] M. Ackermann et al. 2013. Detection of the Characteristic Pion-Decay Signature in Supernova Remnants. *Science Magazine*, 339, 2013. doi: 10.1126/science.1231160.

[3] Stefan Funk. Space and ground based gamma-ray astrophysics. *Annual Review of Nuclear and Particle Science*, 2012. doi: http://www.annualreviews.org/doi/10.1146/annurev-nucl-102014-022036.

[4] Magic observation, 2017. URL http://ihp-lx.ethz.ch/Stamet/magic/magicIntro.html.

[5] G. Simis. Air shower detectors in gamma-ray astronomy. *New journal of physics*, 11, 2009.

[6] A. M. Hisllas. *Journal of physics G. nuclear physics*, 31:95–131, 2005.

[7] J. Knödlseder, M. Mayer, C. Deil, J.-B. Cayrou, E. Owen, N. Kelley-Hoskins, C.-C. Lu, R. Buehler, F. Forest, T. Louge, H. Siejkowski, K. Kosack, L. Gerard, A. Schulz, P. Martin, D. Sanchez, S. Ohm, T. Hassan, and S. Brau-Nogué. GammaLib and ctools. A software framework for the analysis of astronomical gamma-ray data. *aap*, 593:A1, August 2016. doi: 10.1051/0004-6361/201628822.

[8] T K Gaisser. The cosmic-ray spectrum: from the knee to the ankle. *Journal of Physics: Conference Series*, 47(1):15, 2006. URL http://stacks.iop.org/1742-6596/47/i=1/a=002.

[9] F.A. Aharonian. *Very High Energy Cosmic Gamma Radiation: A Crucial Window on the Extreme Universe*. EBSCO ebook academic collection. World Scientific, 2004. ISBN 9789812561732. URL https://books.google.it/books?id=BycD5YpUo7sC.

[10] Stefano Gabici. Gamma-Ray Emission from Supernova Remnants and Surrounding Molecular Clouds, 2017. URL availablefromarXiv:1610.06234[astro-ph.HE].

[11] Ctools user documentation, 2017. URL =http://cta.irap.omp.eu/ctools/users/index.html.

[12] C. J Lagage, P. O. & Cesarsky. The maximum energy of cosmic rays accelerated by supernova shocks. *Astronomy and Astrophysics*, 125(2):249–257, 1983.

[13] S.G. Lucek and A.R. Bell. Non-linear amplification of a magnetic field driven by cosmic ray streaming. *Astrophysics and Space Science*, 272(1):255–262, Jul 2000. ISSN 1572-946X. doi: 10.1023/A:1002656815468. URL https://doi.org/10.1023/A:1002656815468.

[14] H. J. Völk L.O'C Drudy. Hydromagnetic shock structure in the presence of cosmic rays. *Apj*, 248, 1981.

[15] A. et al. Abramowski. Acceleration of petaelectronvolt protons in the Galactic Centre. *Nature*, 531:476–479, March 2016. doi: 10.1038/nature17147. URL http://hal.in2p3.fr/in2p3-01303680. See paper for full list of authors - 29 pages, 7 figures, 3 tables, in press, for official published article see this http URL.

[16] A. R. Bell. Cosmic ray acceleration. *Astroparticle Physics*, 43:56–70, 2013.

[17] H. J. Völk L. O'C Drudy, F. A. Aharonian. The gamma-ray visibility of supernova remnants: a test of cosmic ray origin. *Astronomy and Astrophysics Review*, 287, 1994.

[18] F. W. Stecker. Cosmic gamma rays. *Nasa special publications*, 249, 1971.

[19] Elsa de Cea Del Pozo Diego F.Torres, Ana Y. Rodriguez Marrero. MAGIC J0616+225 as delayed TeV emission of cosmic rays diffusing from the supernova remnant IC 443. *Monthly Notices of the Royal Astronomical Society: Letters*, 387: L59–L63, 2008. doi: http://dx.doi.org/10.1111/j.1745-3933.2008.00485.x.

[20] M. Tavani et al. (2010). MAGIC J0616+225 as delayed TeV emission of cosmic rays diffusing from the supernova remnant IC 443. *Astrophisical journal Letters*, 710(2):L151–L155, 2010. doi: 10.1088/2041-8205/710/2/L151.

[21] A. Guliani et al. (2011). Neutral pion emission from accelerated protons in the supernova remnant w44. *Astrophisical journal Letters*, 742(2):L30, 2011.

[22] F. A. Aharonian, A. M. Atoyan, and T. Kifune. Inverse Compton gamma radiation of faint synchrotron X-ray nebulae around pulsars. *mnras*, 291:162–176, October 1997. doi: 10.1093/mnras/291.1.162.

[23] S. Gabici and F. A. Aharonian. Searching for Galactic Cosmic-Ray Pevatrons with Multi-TeV Gamma Rays and Neutrinos. *apjl*, 665:L131–L134, August 2007. doi: 10.1086/521047.

[24] F. Aharonian, L. Bergström, C. Dermer, R. Walter, and M. Türler. *Astrophysics at Very High Energies: Saas-Fee Advanced Course 40. Swiss Society for Astrophysics and Astronomy*. Saas-Fee Advanced Course. Springer Berlin Heidelberg, 2013. ISBN 9783642361340. URL https://books.google.it/books?id=LdpEAAAAQBAJ.

[25] Acharya et al (2015). The Cherenkov Telescope Array potential for the study of young supernova remnants. *Astroparticle Physics*, 62:152–164, March 2015. doi: 10.1016/j.astropartphys.2014.08.005.

[26] H.E.S.S. Collaboration, A. Abramowski, F. Aharonian, F. A. Benkhali, A. G. Akhperjanian, E. Angüner, G. Anton, S. Balenderan, A. Balzer, A. Barnacka, and et al. TeV γ-ray observations of the young synchrotron-dominated SNRs G1.9+0.3 and G330.2+1.0 with H.E.S.S. *mnras*, 441:790–799, June 2014. doi: 10.1093/mnras/stu459.

[27] F. Aharonian et al. HESS upper limits for Kepler's supernova remnant. *aap*, 488: 219–223, September 2008. doi: 10.1051/0004-6361:200809401.

[28] H. Abdalla et al. Deeper H.E.S.S. Observations of Vela Junior (RX J0852.0-4622): Morphology Studies and Resolved Spectroscopy. 2016.

[29] Gammalib user manual, 2017. URL http://gammalib.sourceforge.net/users/user_manual/index.html.

[30] Ctools documentation, 2017. URL http://cta.irap.omp.eu/ctools-devel/doxygen/index.html.

[31] Gammalib documentation, 2017. URL http://gammalib.sourceforge.net/doxygen/index.html.

[32] J. R Mattox et al. (1996). The Likelihood Analysis of EGRET Data. *Astrophysical Journal*, 461:396–407, 1996.

[33] Oliver Krause, Stephan M. Birkmann, Tomonori Usuda, Takashi Hattori, Miwa Goto, George H. Rieke, and Karl A. Misselt. The cassiopeia a supernova was of type iib. *Science*, 320(5880):1195–1197, 2008. doi: 10.1126/science.1155788.

[34] Decourchell, A. et al. 2001. *A A*, (365):L218, 2001.

[35] V. A. Acciari et al. (2011). Discovery of tev gamma-ray emission from tycho's supernova remnant. *The Astrophysical Journal Letters*, 730(2):L20, 2011. URL http://stacks.iop.org/2041-8205/730/i=2/a=L20.

[36] F. Giordano et al.(2012). Fermi large area telescope detection of the young supernova remnant tycho. *The Astrophysical Journal Letters*, 744(1):L2, 2012. URL http://stacks.iop.org/2041-8205/744/i=1/a=L2.

[37] S. Archambault et al. (2017). Gamma-ray observations of tycho's supernova remnant with veritas and fermi. *The Astrophysical Journal*, 836(1):23, 2017. URL http://stacks.iop.org/0004-637X/836/i=1/a=23.

[38] P. Slane, S.-H. Lee, D. C. Ellison, D. J. Patnaude, J. P. Hughes, K. A. Eriksen, D. Castro, and S. Nagataki. A cr-hydro-nei model of the structure and broadband emission from tycho's supernova remnant. *The Astrophysical Journal*, 783(1):33, 2014. URL http://stacks.iop.org/0004-637X/783/i=1/a=33.

[39] E. G. Berezhko, L. T. Ksenofontov, and H. J. Völk. The nature of gamma-ray emission of tycho's supernova remnant. *The Astrophysical Journal*, 763(1):14, 2013. URL http://stacks.iop.org/0004-637X/763/i=1/a=14.

[40] Xiao Zhang, Yang Chen, Hui Li, and Xin Zhou. On the hadronic -ray emission from tycho's supernova remnant. *Monthly Notices of the Royal Astronomical Society: Letters*, 429(1):L25–L29, 2013. doi: 10.1093/mnrasl/sls016. URL http://dx.doi.org/10.1093/mnrasl/sls016.

[41] Armen Atoyan and Charles D. Dermer. Gamma rays from the tycho supernova remnant: Multi-zone versus single-zone modeling. *The Astrophysical Journal Letters*, 749(2):L26, 2012. URL http://stacks.iop.org/2041-8205/749/i=2/a=L26.

[42] Armen Atoyan and Charles D. Dermer. Gamma rays from the tycho supernova remnant: Multi-zone versus single-zone modeling. *The Astrophysical Journal Letters*, 749(2):L26, 2012. URL http://stacks.iop.org/2041-8205/749/i=2/a=L26.

[43] Pilar Ruiz-Lapuente et al.(2004). The binary progenitor of tycho brahe's 1572 supernova. *Nature Letters*, 431:L1069–L1072, 2004. URL http://www.nature.com/nature/journal/v431/n7012/full/nature03006.html.

[44] E. M. Reynoso, P. F. Velázquez, G. M. Dubner, and W. M. Goss. The environs of tycho's supernova remnant explored through the h i 21 centimeter line. *The Astronomical Journal*, 117(4):1827, 1999. URL http://stacks.iop.org/1538-3881/117/i=4/a=1827.

[45] Jae-Joon Lee, Bon-Chul Koo, and Keni'chi Tatematsu. The environment of tycho: Possible interaction with the molecular cloud. *The Astrophysical Journal Letters*, 605(2):L113, 2004. URL http://stacks.iop.org/1538-4357/605/i=2/a=L113.

[46] Sajan Kumar. A detailed study of Gamma-ray emission from Cassiopeia A using VERITAS. *eprint arXiv:1508.07453*, 2015. doi: http://adsabs.harvard.edu/abs/2015arXiv150807453K.

[47] Una Hwang et al.(2004). A million second chandra view of cassiopeia a. *The Astrophysical Journal Letters*, 615(2):L117, 2004. URL http://stacks.iop.org/1538-4357/615/i=2/a=L117.

[48] J. E. Reed, J. Jeff Hester, and P. F. Fabian, A. C.and Winkler. The three-dimensional structure of the cassiopeia a supernova remnant. i. the spherical shell. 440:706, 1995. doi: http://dx.doi.org/10.1086/175308.

[49] Aharonian, F. et al. (2001). Evidence for tev gamma ray emission from cassiopeia a. *AA*, 370(1):112–120, 2001. doi: 10.1051/0004-6361:20010243. URL https://doi.org/10.1051/0004-6361:20010243.

[50] A. A. Abdo, M. Ackermann, and M. Ajello et al. 2010. Fermi large area telescope first source catalog. *The Astrophysical Journal Supplement Series*, 188(2):405, 2010. URL http://stacks.iop.org/0067-0049/188/i=2/a=405.

[51] Augusto Ghiotto; for The VERITAS Collaboration. A Deep Observation of Gamma-ray Emission from Cassiopeia A using VERITAS. *eprint arXiv:1511.00309*, 2015. doi: http://adsabs.harvard.edu/abs/2015arXiv151100309G.

[52] V. G. Sinitsina and V. Y. Sinitsina. Results of observations of shell supernova remnants at ultrahigh energies with the shalon mirror cherenkov telescopes. *Bulletin of the Lebedev Physics Institute*, 42(6):169–175, Jun 2015. ISSN 1934-838X. doi: 10.3103/S1068335615060032. URL http://dx.doi.org/10.3103/S1068335615060032.

[53] S. H. J. Wallström, C. Biscaro, F. Salgado, J. H. Black, I. Cherchneff, S. Muller, O. Berné, J. Rho, and A. G. G. M. Tielens. CO rotational line emission from a dense knot in Cassiopeia A. Evidence for active post-reverse-shock chemistry. , 558: L2, October 2013. doi: 10.1051/0004-6361/201322576.

[54] Charles D. Kilpatrick, John H. Bieging, and George H. Rieke. A systematic survey for broadened co emission toward galactic supernova remnants. *The Astrophysical Journal*, 816(1):1, 2016. URL http://stacks.iop.org/0004-637X/816/i=1/a=1.

[55] G. G. Pavlov, D. Sanwal, and M. A. Teter. Central Compact Objects in Supernova Remnants. In F. Camilo and B. M. Gaensler, editors, *Young Neutron Stars and Their Environments*, volume 218 of *IAU Symposium*, page 239, 2004.

[56] F. Acero, M. Lemoine-Goumard, M. Renaud, J. Ballet, J. W. Hewitt, R. Rousseau, and T. Tanaka. Study of TeV shell supernova remnants at gamma-ray energies. , 580:A74, August 2015. doi: 10.1051/0004-6361/201525932.

[57] W. Baade. Nova ophiuchi of 1604 as a supernova. *The Astrophysical Journal*, 97: 119, 1943. doi: http://dx.doi.org/10.1086/144505.

[58] Stephen P. Reynolds, Kazimierz J. Borkowski, Una Hwang, John P. Hughes, Carles Badenes, J. M. Laming, and J. M. Blondin. A deep chandra observation of kepler's supernova remnant: A type ia event with circumstellar interaction. *The Astrophysical Journal Letters*, 668(2):L135, 2007. URL http://stacks.iop.org/1538-4357/668/i=2/a=L135.

[59] J. B. Doggett and D. Branch. A comparative study of supernova light curves. , 90: 2303–2311, November 1985. doi: 10.1086/113934.

[60] Jacco Vink. The kinematics of kepler's supernova remnant as revealed by chandra. *The Astrophysical Journal*, 689(1):231, 2008. URL http://stacks.iop.org/0004-637X/689/i=1/a=231.

[61] Satoru Katsuda, Koji Mori, Keiichi Maeda, Masaomi Tanaka, Katsuji Koyama, Hiroshi Tsunemi, Hiroshi Nakajima, Yoshitomo Maeda, Masanobu Ozaki, and Robert Petre. Kepler's supernova: An overluminous type ia event interacting with a massive circumstellar medium at a very late phase. *The Astrophysical Journal*, 808(1): 49, 2015. URL http://stacks.iop.org/0004-637X/808/i=1/a=49.

[62] Hiroya Yamaguchi et al.(2014). Discriminating the progenitor type of supernova remnants with iron k-shell emission. *The Astrophysical Journal Letters*, 785(2):L27, 2014. URL http://stacks.iop.org/2041-8205/785/i=2/a=L27.

[63] R. Sankrit, W. P. Blair, T. Delaney, L. Rudnick, I. M. Harrus, and J. A. Ennis. HST/ACS imaging of a Balmer-dominated shock in Keplers supernova remnant. *Advances in Space Research*, 35:1027–1030, 2005. doi: 10.1016/j.asr.2004.11.018.

[64] Pilar Ruiz-Lapuente. The light curve and distance of the kepler supernova: News from four centuries ago. *The Astrophysical Journal*, 842(2):112, 2017. URL http://stacks.iop.org/0004-637X/842/i=2/a=112.

[65] Ravi Sankrit et al.(2016). Second epoch hubble space telescope observations of kepler's supernova remnant: The proper motions of balmer filaments. *The Astrophysical Journal*, 817(1):36, 2016. URL http://stacks.iop.org/0004-637X/817/i=1/a=36.

[66] Helder et al.(2012). Observational signatures of particle acceleration in supernova remnants. *Space Science Reviews*, 173(1):369–431, Nov 2012. doi: 10.1007/s11214-012-9919-8. URL http://dx.doi.org/10.1007/s11214-012-9919-8.

[67] E. G. Berezhko, L. T. Ksenofontov, and H. J. Völk. Gamma-ray emission expected from Kepler's supernova remnant. *aap*, 452:217–221, June 2006. doi: 10.1051/0004-6361:20064801.

[68] R. Enomoto et al. (2008). Cangaroo-iii search for gamma rays from kepler's supernova remnant. *The Astrophysical Journal*, 683(1):383, 2008. URL http://stacks.iop.org/0004-637X/683/i=1/a=383.

[69] R. Capelli, R. S. Warwick, N. Cappelluti, S. Gillessen, P. Predehl, D. Porquet, and S. Czesla. Discovery of X-ray flaring activity in the Arches cluster. , 525:L2, January 2011. doi: 10.1051/0004-6361/201015758.

[70] Q. Daniel Wang, Hui Dong, and Cornelia Lang. The interplay between star formation and the nuclear environment of our galaxy: deep x-ray observations of the galactic centre arches and quintuplet clusters. *Monthly Notices of the Royal Astronomical Society*, 371(1):38–54, 2006. doi: 10.1111/j.1365-2966.2006.10656.x. URL +http://dx.doi.org/10.1111/j.1365-2966.2006.10656.x.

[71] Yuta Asahina, Tomohisa Kawashima, Naoko Furukawa, Rei Enokiya, Hiroaki Yamamoto, Yasuo Fukui, and Ryoji Matsumoto. Magnetohydrodynamic simulations of the formation of molecular clouds toward the stellar cluster westerlund 2: Interaction of a jet with a clumpy interstellar medium. *The Astrophysical Journal*, 836 (2):213, 2017. URL http://stacks.iop.org/0004-637X/836/i=2/a=213.

[72] G. Maurin, A. Marcowith, N. Komin, F. Krayzel, and G. Lamanna. Embedded star clusters as sources of high-energy cosmic rays . Modelling and constraints. , 591: A71, June 2016. doi: 10.1051/0004-6361/201628465.

[73] H.E.S.S. Collaboration, A. Abramowski, and F. et al. (2011) Acero. Very-high-energy gamma-ray emission from the direction of the Galactic globular cluster Terzan 5. , 531:L18, July 2011. doi: 10.1051/0004-6361/201117171.

[74] Ruo-Yu Liu, Xiang-Yu Wang, Anton Prosekin, and Xiao-Chuan Chang. Modeling the gamma-ray emission in the galactic center with a fading cosmic-ray accelerator. *The Astrophysical Journal*, 833(2):200, 2016. URL http://stacks.iop.org/0004-637X/833/i=2/a=200.

[75] Aharonian et al.(2009). Spectrum and variability of the Galactic center VHE γ-ray source HESS J1745-290. , 503:817–825, September 2009. doi: 10.1051/0004-6361/200811569.

[76] F. Yusef-Zadeh et al.(2013). Interacting cosmic rays with molecular clouds: A bremsstrahlung origin of diffuse high-energy emission from the inner $2^o x 1^o$ of the

galactic center. *The Astrophysical Journal*, 762(1):33, 2013. URL http://stacks.iop.org/0004-637X/762/i=1/a=33.

[77] K. Bernlöhr et al. Monte carlo design studies for the cherenkov telescope array. *Astroparticle Physics*, 43:171 – 188, 2013. ISSN 0927-6505. doi: http://dx.doi.org/10.1016/j.astropartphys.2012.10.002. URL http://www.sciencedirect.com/science/article/pii/S0927650512001867. Seeing the High-Energy Universe with the Cherenkov Telescope Array - The Science Explored with the CTA.

[78] V.V. Bugayov S.R. Kelner, F.A. Aharonian. Energy spectra of gamma rays, electrons, and neutrinos produced at interactions of relativistic protons with low energy radiation. *Phys. Rev. D*, 78:034013, Aug 2008. doi: 10.1103/PhysRevD.78.034013. URL https://link.aps.org/doi/10.1103/PhysRevD.78.034013.

[79] Damiano Caprioli. Cosmic-ray acceleration in supernova remnants: non-linear theory revised. *Journal of cosmology and astroparticle physics*, 2012, 2012.

[80] Albert, J. et al (2007). Observation of VHE γ-rays from Cassiopeia A with the MAGIC telescope. , 474:937–940, November 2007. doi: 10.1051/0004-6361:20078168.

[81] L. Saha, T. Ergin, P. Majumdar, M. Bozkurt, and E. N. Ercan. Origin of gamma-ray emission in the shell of Cassiopeia A. *aap*, 563:A88, March 2014. doi: 10.1051/0004-6361/201323218.

[82] Yajie Yuan, Stefan Funk, Gülauger Jóhannesson, Joshua Lande, Luigi Tibaldo, and Yasunobu Uchiyama. Fermi large area telescope detection of a break in the gamma-ray spectrum of the supernova remnant cassiopeia a. *The Astrophysical Journal*, 779(2):117, 2013. URL http://stacks.iop.org/0004-637X/779/i=2/a=117.

[83] S. S. Wilks. The large-sample distribution of the likelihood ratio for testing composite hypotheses. *Ann. Math. Statist.*, 9(1):60–62, 03 1938. doi: 10.1214/aoms/1177732360. URL http://dx.doi.org/10.1214/aoms/1177732360.

[84] Archambault et al. 2017. Gamma-ray observations of tycho's supernova remnant with veritas and fermi. *The Astrophysical Journal*, 836(1):23, 2017. URL http://stacks.iop.org/0004-637X/836/i=1/a=23.

[85] E. M. Reynoso & W. M. Goss. A new determination of the distance to kepler's supernova remnant. *The Astronomical Journa*, 118:926–929, 1999. doi: http://dx.doi.org/10.1086/300990.

[86] F. Acero et al.(2017). Prospects for cherenkov telescope array observations of the young supernova remnant rx j1713.73946. *The Astrophysical Journal*, 840(2):74, 2017. URL http://stacks.iop.org/0004-637X/840/i=2/a=74.

[87] Y. Uchiyama et al. 2007. Extremely fast acceleration of cosmic rays in a supernova remnant. *Nature Letters*, 449:L576–l578, 2007. doi: doi:10.1038/nature06210.

[88] E. A. et al.2012 Helder. Observational signatures of particle acceleration in supernova remnants. *Space Science Reviews*, 173(1):369–431, Nov 2012. doi: 10.1007/s11214-012-9919-8. URL http://dx.doi.org/10.1007/s11214-012-9919-8.

[89] Bernlöhr, K et al.2012. Monte carlo design studies for the cherenkov telescope array. 43, 10 2012.